



“BABEȘ-BOLYAI” UNIVERSITY, CLUJ-NAPOCA
FACULTY OF PHYSICS
PHYSICAL DOCTORAL SCHOOL

Physical and chemical degradation studies
on polymeric systems
PhD Thesis Summary

Scientific advisor:
Prof. dr. Mihai Todica

PhD Student:
Carmen Rodica Niculăescu

Cluj-Napoca
2022

CONTENT

Summary	4
Chapter 1: Introduction	
1.1. Polymeric materials	7
1.1.1. Polystyrene (PS)	10
1.1.2. Polyethylene terephthalate (PET)	11
1.2. Human teeth: enamel (FS) and dentin (FD)	12
Chapter 2: Degradation methods	
2.1. Thermal degradation	14
2.1.1. Thermal degradation in polystyrene (PS) samples	15
2.1.2. Thermal degradation in polyethylene terephthalate (PET) samples	15
2.2. Exposure to gamma radiation	16
2.2.1. Radiative degradation in polystyrene (PS) samples	17
2.2.2. Radiative degradation in polyethylene terephthalate (PET) samples	17
2.3. Exposure to chemical agents	
2.3.1. Chemical degradation of enamel and dentin in human teeth	18
Chapter 3: Physical methods of investigation	
3.1. X-ray diffraction (XRD)	20
3.2. Fourier Transform Infrared Spectroscopy (FT-IR)	25
3.3. Differential thermal and thermogravimetric analysis (DTA / TGA)	29
3.4. UV-VIS Spectroscopy and Fluorescence	31
Chapter 4: Experimental results - PS	
4.1. Visual analysis	33
4.2. TG and DTA analysis	34
4.3. XRD analysis	37
4.3.1. Analysis of thermally degraded commercial PS samples	37
4.3.2. Analysis of thermally degraded and then gamma irradiated PS samples	41
4.4. FT-IR analysis	44
4.5. UV-VIS Analysis and Fluorescence	47
4.6. Conclusions	52
Chapter 5: Experimental results - PET	
5.1. XRD analysis	54
5.1.1. Analysis of thermally degraded commercial PET samples	54
5.1.2. Analysis of thermally degraded and then gamma irradiated PET samples	58
5.2. DTA analysis	64
5.3. Conclusions	66
Chapter 6: Experimental results - FS and FD	
6.1. XRD analysis	67
6.2. FT-IR analysis	73
6.3. Conclusions	77
Chapter 7: Final Conclusions	79
Selected references	85
Keywords: polyethylene terephthalate, human teeth, degradation, structural analysis, XRD, FT-IR, UV-VIS, DTA / TG.	
ANNEX 1. PUBLISHED WORKS	89
ANNEX 2. PARTICIPATIONS IN CONFERENCES	90

Chapter 1: Introduction

1.1. Polymeric materials

One of the current concerns of plastic packaging suppliers is the production of "green packaging", recyclable and with the lowest possible pollution rate. For these reasons, research into the replacement of polymeric materials is currently being accelerated and aims, in particular, to obtain new materials that are easily recyclable and with a residual percentage as low as possible. We are looking for cheap and efficient degradation and recycling solutions, such as heat, chemical and radiative treatments. By applying these treatments, the morphology and even the chemical structure of the polymers can be modified, sometimes leading to the appearance of unwanted compounds. That is why investigating these effects is an essential step in recycling. Given the large quantities of polymeric materials that are produced and used daily around the world, the replacement or recycling of these materials is a pressing and necessary issue, which is why we consider that the study presented in this paper is current.

Among the general purpose polymers, we studied polystyrene and polyethylene terephthalate, and for biological systems, we chose human teeth - enamel, and dentin.

Polystyrene (PS)

Polystyrene is a synthetic compound with the chemical formula $(C_8H_8)_n$ (Fig 1.2), discovered by the German Eduard Simon in 1839. This compound belongs to the class of synthetic polymers of aromatic hydrocarbons, based on the styrene monomer - a simple, liquid hydrocarbon, obtained from oil. Styrene also occurs naturally in foods such as cinnamon, strawberries, coffee, or beef. (www.chemicalsafetyfacts.org)

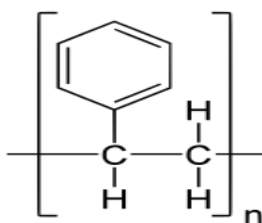


Figure 1.2. Structural formula for PS.

Polystyrene is obtained by the polymerization reaction of styrene, through which the carbon-carbon bond π of the vinyl group is broken and the carbon-carbon bond σ is formed, attaching to the carbon of another styrene monomer. Polystyrene has a molecular weight between 100,000 - 400,000 g / mol and a melting temperature of around 240 °C. From a structural point of view, polystyrene is an amorphous or partially crystalline polymer material and thermally workable (thermoplastic). At room temperature, it is in the solid state, but becomes a viscous fluid if heated above its glass transition temperature of about 100 °C (softening temperature) and returns to the solid-state after cooling. Due to this thermal behavior, this material can be processed by extrusion and casting in different shapes. Naturally, polystyrene is transparent but can be colored with dyes depending on its uses. It is insoluble, which makes this

polymer have applications in a wider field, ranked among the most versatile plastics used in the manufacture of consumer products, being produced worldwide in quantities of millions of tons. In the form of solid plastic, it is used for food packaging, the manufacture of laboratory utensils, the manufacture of cases for electronic devices, toys, etc. By extrusion, it can be transformed into an expanded material widely used in the insulation of buildings, protective packaging, car parts, road stabilization systems, etc. According to International Standards (ASTM - American Materials Testing Society), polystyrene is not considered a biodegradable material, its shelf life is estimated at over 40 years. Its use, in particular, in the form of foam, leads to large accumulations of waste causing a very high degree of pollution of nature, and at the same time reducing the survival rate of marine and indirectly human fauna. In terms of degradation, polystyrene ranks second after glass, as it is affected only by mechanical action or radiation exposure.

1.1.2. Polyethylene terephthalate (PET)

Polyethylene terephthalate has the chemical formula $(C_{10}H_8O_4)_n$ and belongs to the category of thermoplastic polyesters, polymers containing the ester group (-CO-O-). (Fig. 1.3) It was first synthesized in the 1940 by chemists at DuPont seeking to develop polymeric materials for the manufacture of textiles.

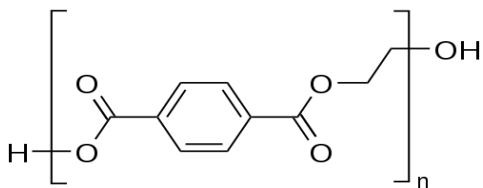


Figure 1.3. The structural formula of PET.

Polyethylene terephthalate is a colorless, transparent, and semi-crystalline material obtained by polycondensation of dimethyl terephthalate (terephthalic acid) with ethylene glycol. It is a thermoplastic polyester that becomes liquid at a temperature of about 260 °C. Heated to its melting point and then cooled, the material does not suffer significant degradation. PET has different degrees of crystallinity and different mechanical properties and is usually provided in the form of granules, compounds with or without filler, and in the form of powders. Commercially, we also meet it under other names such as PETG, PETE, or PETT. This glycol-enhanced polymer (called PETG) is more resistant to wear, so it is used in the manufacture of water containers, clothing fibers, etc. Combined with other materials, such as fiberglass or carbon nanotubes, it gives rise to materials with increased strength. In solid form, it is used in approximately 90% of food packaging or liquid storage containers. It is an economical plastic, but relatively difficult to recycle.

For example, plastic film - used for packaging products, is heated to a melting point of 260 °C and then cooled and does not suffer significant degradation, which leads to a continuous and massive accumulation of waste nationally and globally. The percentage of recycling is small, which places it in the ranking of the most polluting material produced by humanity. This is one of the reasons why scientists are constantly investigating the potential for recycling/degradation of PET products.

1.2. Human teeth: enamel (FS) and dentine (FD)

TEETH are a bony component of the human body made up mostly of natural hydroxyapatite (HA), a complex compound that contains calcium, phosphorus, oxygen and hydrogen atoms, and has the chemical formula $\text{Ca}_{10}(\text{PO}_4)_6(\text{OH})_2$ [1-3]. The main components of a tooth are the crown and the root. The crown is protected by a thin layer called ENAMEL, which contains under it a hard tissue that protects the dental pulp, called DENTINE.

Hydroxyapatite represents 96% of the enamel volume and 74% of the dentin volume, respectively [4] and is found in the structure of the human tooth both in the amorphous phase and in the crystalline phase. The structure of a tooth can change under the action of various aggressive external agents such as food composition, thermal shocks or chemical shocks. [5]

Enamel is the hardest tissue in the human body, and contains mineral crystals (hydroxyapatite) but also water in a proportion of 1–6% of the mass of enamel.

Dentine is the main supporting structure of the tooth being covered with enamel, and is responsible for the color of the teeth, containing between 15–30% water from its mass. [6]

In addition to the organic material, the teeth also contain other inorganic components such as CO_3^{2-} . carbonate ions. They are located in the tetrahedron PO_4^{3-} and represent up to 3.5% of the enamel mass and up to 5.6% of the dentin mass [7, 8]. If the dentin is associated with the vital part of the tooth, the enamel acts as a protector against the negative action of external factors such as food, acidic fluids, or other substances that enter the oral cavity through food and often have an aggressive action on the tooth structure.

Substances present in food that have an aggressive effect on the teeth include citric acid and acetic acid contained in fruits or other foods consumed. In addition to food, teeth can come into contact with other chemicals, such as substances used in teeth whitening procedures that contain carbamide peroxide, which can degrade enamel or dentin. [9] Enamel usually provides sufficient protection for dentin when the substances are in low concentration and the exposure time is relatively short. As a result of too frequent or incorrect dental procedures, the enamel or dentin part can be severely damaged. The degradation phenomenon caused by exposure to chemicals in the diet is an important aspect because, by degradation, the tooth surfaces are less resistant to the physical forces that occur during mastication. [5] There are various studies investigating the action of certain acids on teeth, [10 -13] but investigation by complementary physicochemical methods such as X-ray diffraction and FT-IR spectroscopy, is less present in the literature. Given this aspect, we proposed to use these methods in the study of the repeated effect of citric acid, a chemical agent present in the daily diet.

Chapter 2: Degradation methods

2.1. Thermal degradation

Heat treatment is a process that changes the temperature of the material, being accompanied by physicochemical events that can change its properties at the macro- and microscopic levels. Thermal degradation is the simplest method of destroying polymeric materials but its use could produce unwanted and polluting products for the environment. [14, 15] In the case of polymers, thermal degradation can cause structural changes and even the appearance of unwanted by-products. Energy absorption can cause irreversible changes in the physicochemical properties of materials through oxidation phenomena [16-20]. Thermal degradation also depends on the heating-cooling rate of the material, which can lead to the partial or total destruction of the structure or even crystallization. [21] In the case of the samples in this study, the heating process was applied to a certain temperature, using a Nabertherm LHT 08/16, 8 l, 1600 °C high-temperature heating oven, followed by slow cooling. The samples placed in ceramic crucibles were heated from ambient temperature to 350 °C with a temperature rise rate of 10 °C / min, then allowed to cool slowly to room temperature, without any other external action to accelerate cooling.

2.1.1. Thermal degradation in polystyrene samples PS

The aim of the study was to identify structural changes caused by the degradation of polystyrene by heating at various temperatures and by irradiation with gamma radiation.

Sample preparation

Set 1: Twenty samples of commercial polystyrene were cut from the packaging of some commercial products, weighing about 500 mg each. These non-heat treated commercial polystyrene samples were labeled PS.

Set 2: Six samples of polystyrene, initially PS, were heated in ceramic crucibles on an electric hob for 30 minutes, at five temperature values: 140 °C, 200 °C, 250 °C, 300 °C, and 350 °C. The process of heating the samples took about 30 minutes, and after reaching the desired temperature, they were taken from the hob and allowed to cool slowly in the air to ambient temperature (approximately 20 °C). These heat-treated polystyrene samples were marked with PS 140 °C, PS 200 °C, PS 250 °C, PS 300 °C and PS 350 °C.

2.1.2. Thermal degradation of PET polyethylene terephthalate samples

Polyethylene terephthalate is one of the largest pollutants in the class of household and industrial polymers, being a material used in the manufacture of most food and liquid storage containers. At present, the continuous accumulation of PET waste and the low recycling rate of products from this material is worrying, which is why there is permanent pollution of the environment in which we live. One of the simplest methods of recycling / reconditioning PET products is thermal degradation. Although it is a simple method, it has certain shortcomings because most of the time, the degradation also results in reaction by-products, which are in turn pollutants to the environment. [14] Structural investigation and the identification of different processes of degradation of this material are concerns worldwide.

For these reasons, the main objective of this study was to identify structural changes caused by the degradation of polyethylene terephthalate samples by applying heat treatment, followed by a slow cooling process. Another objective was to establish the effects of irradiation on the structure of PET materials if they were exposed to gamma radiation and absorbed different doses of radiation.

Sample preparation

Two sets of PET samples cut from containers in which water was bottled were prepared. These square-shaped samples, measuring 20 x 20 mm and 0.3 mm thick, were washed several times with alcohol and distilled water, then dried at room temperature in places free of dust or other impurities. The samples were analyzed both in the initial state and after the thermal degradation process.

Set 1: Initial, untreated PET samples were marked with **G00 initial**.

Set 2: Three of the initial samples (initial G00) were placed in ceramic crucibles and gradually heated on an electric hob to a temperature of 300 °C. In order to obtain a homogeneous melt, they were kept at this temperature for 1-2 minutes. After this stage, they were allowed to cool progressively by passive convection, at room temperature, thus obtaining samples of the same size and thickness. These samples were marked with **G00 melted-cooled**.

2.2. Gamma radiation exposure

Gamma electromagnetic radiation comes from the radioactive decay of atomic nuclei and consists of high-energy photons. It was discovered in 1900 by Paul Villard, and three years later in 1903, Ernest Rutherford named it gamma rays, due to their penetrating properties of matter. The behavior of polymers at high gamma exposure of hundreds of kGy is described in various studies, but these effects are not common because structural changes are caused by the breaking of the polymer bond after irradiation. [24-27] Gamma electromagnetic radiation comes from the radioactive decay of atomic nuclei and consists of high-energy photons. It was discovered in 1900 by Paul Villard, and three years later in 1903, Ernest Rutherford named it gamma rays, due to their penetrating properties of matter. The behavior of polymers at high gamma exposure of hundreds of kGy is described in various studies, but these effects are not common because structural changes are caused by the breaking of the polymer bond after irradiation. [24-27] A number of studies address the properties of polymers depending on the dose and nature of the sample, but there is little work in the literature on the combined effect of gamma irradiation at moderate doses with the thermal degradation process, which is why we have focused on this direction. Since 2011 it has been shown that the gamma irradiation of some polymeric materials induces crystallization [16, 28], possible ionization and breaking of the chemical bonds of the polymer chains. The maximum accepted irradiation dose is about 25 kGy, while for food pasteurization the accepted doses are between 2 - 10 kGy. [Safety and nutritional adequacy of irradiated food, World Health Organization Geneva 1994]

In this study, the gamma radiation came from a ⁶⁰Co source (Gamma 900 Camera), with fluency of 3.46 Gy / h and a uniform radiation density. Dose flow calibration was performed by ferrous sulfate dosimetry in Gy/h.

2.2.1. Radiative degradation in polystyrene (PS) samples

Several samples from commercial polystyrene and the set of thermally degraded polystyrene were exposed to gamma irradiation for about 3 months.

Set 1: A sample of unheated commercial polystyrene (PS) was exposed to gamma radiation and the irradiated sample was marked with **PSI**.

Set 2: Five polystyrene samples that were subsequently thermally degraded at temperatures between 140 - 350 °C (**PS 140 °C**, **PS 200 °C**, **PS 250 °C**, **PS 300 °C**, and **PS 350 °C**) were exposed to gamma radiation, and the results of the sample were named with **PSI 140 °C**, **PSI 200 °C**, **PSI 250 °C**, **PSI 300 °C**, and **PSI 350 °C**.

2.2.2. Radiative degradation in polyethylene terephthalate (PET) samples

For the study of the effect of irradiation on PET material, samples of commercial PET and samples of PET thermally degraded were selected, which were then exposed to gamma radiation for different time intervals so that the samples absorb different radiation doses, namely: 456 Gy, 3 kGy and 7 kGy. The values of these doses were established based on previous studies performed on polymeric materials that had properties comparable to those of the materials used in this study, results that showed the possibility of changes by radiation exposure at doses between 400 Gy - 7 KGy.

Set 1: Three untreated PET samples (initial G00) were exposed to gamma radiation for different times, and the resulting samples were marked with **G00 456 Gy**, **G00 3kGy** and **G00 7kG**.

Set 2: Three PET samples previously melted at 300 °C (**melted-cooled G00**) were exposed to gamma radiation for different times, so that the samples absorb the three doses of the selected radiation 456 Gy, 3 kGy and 7 kGy. The resulting samples were denoted with irradiated **G01 melted-cooled irradiated 456 Gy**, **G02 melted-cooled irradiated 3 kGy** and **G03 melted-cooled irradiated 7 kGy**.

2.3. Exposure to chemical agents

2.3.1. Chemical degradation in human teeth samples

The aim of the study was to identify structural changes due to the degradation action of citric acid (CI) in samples taken from a human tooth.

Sample preparation

Set 1: Six samples were taken from two human molars (M), selected without caries or cracks and provided by a dental office. The teeth were cut longitudinally parallel to the side face, resulting in two sets of samples with different parts, namely: two samples with enamel on the outside - called facets with enamel (**FS**) and two samples with the inside of dentin - called facets with dentin (**FD**).

Set 2: Two samples with enamel and two samples with dentin were immersed in pure citric acid solution, with a concentration of 96 %, for a period of four days. This high concentration of citric acid was used to check the behavior of tooth samples in extreme conditions. The samples were named **FS-4dCI**, and **FD-4dCI** respectively.

Set 3: After chemical degradation of the tooth samples in citric acid for four days, two of them were removed, washed with distilled water and left at room temperature in closed containers for 30 days in the dark. This experiment was performed to check whether after the cessation of the action of the chemical agent - citric acid, there are phenomena of relaxation in the structure of the teeth. The 30-day relaxed samples were named **FS-4dCI + 30dRT** and **FD-4dCI + 30dRT**, respectively.

Set 4: Two samples with enamel veneer and another two with dentin veneer were immersed in pure citric acid solution at a concentration of 96% for a period of eight days. The resulting samples were named **FS-8dCI** and **FD-8dCI**, respectively.

In the analysis and characterization of the samples in this study, complementary methods were applied, namely X-ray diffraction, FT-IR infrared spectroscopy, UV-VIS and fluorescence spectroscopy, DTA-TG thermal analysis. These methods will be briefly described in Chapter 3 of this paper.

Chapter 3: Physical methods of investigation

In order to identify possible structural changes, of local order, which may occur after the process of thermal degradation or irradiation of materials, the samples under study were investigated - both before degradation and after heat treatment or after gamma irradiation - by several complementary methods: X-ray diffraction (XRD), thermal analysis (DTA, TG), infrared spectroscopy (FT-IR), UV-VIS and fluorescence spectroscopy.

Chapter 4: Experimental results - PS

4.1. Visual analysis

Polymers are amorphous materials with a low degree of ordering [20, 36] but, under certain conditions, may include small amounts of water or solvent in their structure, which would lead to a local rearrangement of the polymer chain. By heating, these molecules can be removed by evaporation, a phenomenon that is accompanied by a variation in the weight of the sample. If the sample is heated to higher temperatures, certain parts of the sample may be oxidized, resulting in chemical compounds other than the original polymer. These compounds can be removed by degassing, a process that is also accompanied by a mass loss of sample.

The polystyrene samples - from set 2, heated in the temperature range 22 - 350 °C, were visually examined to highlight possible color changes. At the same time, a possible change in their weight was checked. The observations were noted in Table 4.1.

Table 4.1. Experimental data after heating of the samples to the selected temperatures.

Sample name	Initial weight [mg]	Final weight [mg]	Temperature [°]	Color
PS	500	500	22	White
PS 140°C	500	500	140	White
PS 200°C	500	492	200	White Gray
PS 250°C	500	470	250	Gray
PS 300°C	500	440	300	Dark black
PS 350°C	500	400	350	Black

From the analysis of experimental data from Table 4.1., it is found that starting with 200 °C there are changes in the color and mass of the polystyrene samples. The highest weight loss is observed for the sample heated to 350 °C.

4.2. TG and DTA analysis

The data of the visual analysis from Table 4.1. were represented graphically by a curve as a function mass = f (T) and is shown in Figure 4.1. From the analysis of the TG thermogravimetric curve in Figure 4.1., it is observed that the mass loss in the analyzed sample increases with increasing temperature as follows:

- between 22 - 140 °C there are no weight loss variations, the sample is thermally stable.
- between 140 - 200 °C the weight loss is 1.6%, an event associated with the evaporation of water and residual solvents included in the polymer matrix.
- between 200 - 300 °C the weight loss occurred in two stages: the first of 6% and the second of 12%, losses associated with the decomposition of the polymer.
- between 300 - 350 °C the weight loss is more pronounced, by 20%, resulting in accordance with the visual observations which showed that above 300 °C the samples begin to darken and lose more weight.

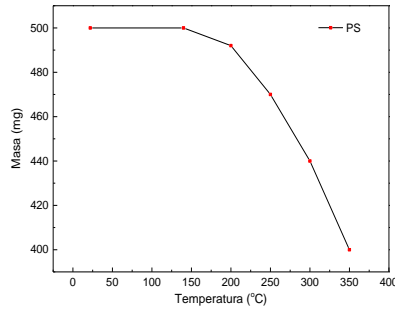


Figure 4.1. TG analysis for polystyrene in the temperature range 20 - 350°C.

The experimental results show that the largest mass loss has the sample heated to 350 °C, which is why the polystyrene samples with the simultaneous DTA / TGA analyzer were investigated. For the measurements, two samples were selected: one sample made of non-irradiated commercial polystyrene (set 1) and the other made of irradiated commercial polystyrene (set 3), heated with a constant rate of temperature rise between 22 and 350 °C. From the comparison of the simultaneous thermal analysis curves DTA / TGA (Fig. 4.2.) obtained from the measurements of the samples of unheated commercial polystyrene (Fig.4.2.a) and on preheated polystyrene up to 350 °C (Fig. 4.2.b) it is observed that they behave differently.



Figure 4.2. DTA / TGA curves for: (a) unheated polystyrene (PS) and (b) polystyrene heated to 350 °C (PS 350 °C).

The thermal events that appear in each of the samples analyzed by DTA / TG, during heating (with the analyzer) with constant speed from ambient temperature up to 600 °C, are presented in Table 4.2.

The thermal and thermogravimetric analysis were in accordance with the resulting visual observations which confirmed that below the temperature of 140 °C the samples are stable, but above this temperature the decomposition of the polymer chain and the oxidation process takes place.

Table 4.2. DTA / TG thermal analysis of PS and PD 350 °C samples

Sample	Temp range	Tmax (DTA)	Δm (TG)	Associated event
PS	25 – 200 °C	Tendo = 116 °C	-	Melting
	200 – 250 °C	Tendo = 216°C	3%.	Melting, decomposition
	250 – 350 °C	Tendo = 333°C	20%	Decomposition
	350 – 500 °C		79%	Degradation decomposition
S 350 °C	25 - 250 °C	Tendo = 126°C Tendo = 223°C	6%	Melting simultaneously with decomposition
	250 – 350 °C	Texo=327°C	83%	Transition in the crystalline phase with decomposition
	350-500°C	Tendo=445°C	17%	Decomposition, degradation

4.3. XRD analysis

In the case of polystyrene, the samples subjected to two degradation processes were investigated: simple thermal degradation of non-irradiated samples and thermal degradation of gamma irradiated samples. To investigate the effects of the two types of degradation in polystyrene, analysis was first performed on irradiated polystyrene samples and then on irradiated samples.

4.3.1 Thermally degraded unirradiated polystyrene

XRD measurements were performed on the commercial polystyrene samples in the initial state, and on the five samples (from set 3) made of polystyrene heated to temperatures of 150 °C, 200 °C, 250 °C, 300 °C and 350 °C, respectively. The diffractograms obtained on the heated samples were compared with the diffractogram of the unheated commercial polystyrene (PS) sample and are shown in Figure 4.3.

Although the overall appearance of the diffractograms appears to be the same, a detailed analysis reveals a revolution in the shape of their parameters as a function of temperature. As a general characteristic, the presence of a wide peak is noticed, centered around $2\theta = 17.8^\circ$, whose amplitude depends on the heat treatment. The shape of this peak suggests the existence of an important amorphous phase fraction in the sample structure.

From Figure 4.3., it is observed that the amplitude of the maximum diffraction peak undergoes changes in intensity. Thus, by heating the samples to 140 °C, 200 °C and 250 °C, the amplitude increases due to the increase of the crystalline phase, compared to the samples heated to 300 °C and 350 °C, where the amplitude decreases, which shows a massive degradation of the polymer at these temperatures.

Heating polystyrene to temperatures above 200 °C has the effect of rearranging the polymer chains into a more orderly structure which leads to an increase in the crystalline phase. [1, 36, 38, 39]

In conclusion, it can be stated that as the samples are heated to temperatures between 250 - 350 °C, the position of the maximum diffraction moves to higher values $2\theta = 19.2^\circ$, and the intensity and area of the diffraction peaks decrease due to the destruction of the ordered phase of polystyrene by oxidation.

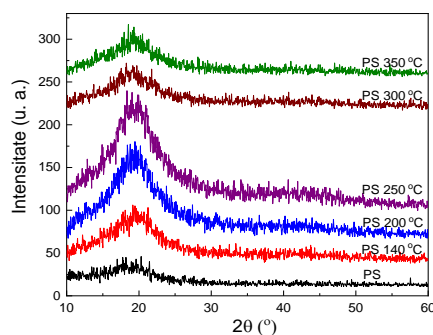


Figure 4.3. Diffractogram of initial-unheated polystyrene (PS) compared with the diffractograms of the heated polystyrene samples.

Table 4.3. presents the comparison between the interplanar distances calculated based on the Bragg equation at the maximum diffraction angles which correspond to each sample analyzed after the heat treatment.

Table 4.3. The interplanar distances calculated for heat-treated polystyrene samples

Non-irradiated samples	2θ (°)	d(Å)
Initial PS	17.8°	4.98 Å
PS 140 °C	17.8 °	4.98 Å
PS 200 °C	18.7°	4.74 Å
PS 250 °C	18.7°	4.74 Å
PS 300 °C	19.5°	4.55 Å
PS 350 °C	19.5°	4.55 Å

4.3.2. Thermally degraded and gamma irradiated polystyrene

Following the absorption of gamma radiation, it is possible to pass some atoms from the chemical bonds of the polymer chains in excited states, the polymer chain may break, which will lead to the local reorganization of the entire molecular assembly.

The irradiated samples, subsequently heated to temperatures of 140 °C, 200 °C, 250 °C, 300 °C, and 350 °C, were analyzed by X-ray diffraction.

From the comparison of the diffractograms obtained on the initial polystyrene sample (unirradiated unheated PS) and the irradiated and unheated sample (PSI) (Fig. 4.4.) it was observed that both diffractograms have a wide peak characteristic of amorphous materials, but in the irradiated sample it is slightly displaced from the value $2\theta = 17.8^\circ$ - in the case of the non-irradiated sample, to $2\theta = 19^\circ$ in the case of the irradiated sample.

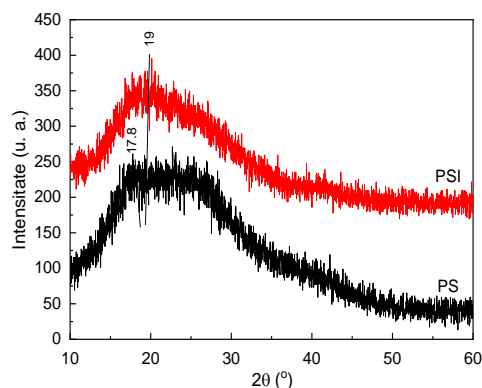


Figure 4.4. XRD diffractograms of non-irradiated polystyrene (PS) and of irradiated polystyrene (PSI). (punct)

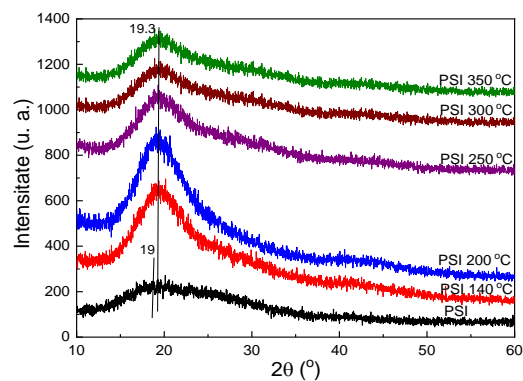


Figure 4.5. XRD diffractogram of irradiated polystyrene (PSI) compared to diffractograms of polystyrene samples heated between and then irradiated.

Figure 4.5. show the diffractograms of the initial irradiated polystyrene (PSI) sample and of the heated and then irradiated samples (PSI 140 °C, PSI 200 °C, PSI 250 °C, PSI 300 °C, PSI 350 °C).

The samples treated at 140 °C, 200 °C, 250 °C and afterwards gamma irradiated show a behavior similar to samples treated but non-irradiated. The interplanar distances for the samples non-heated / heated and gamma irradiated were calculated based on the Bragg equation. The data are presented in Table 4.4.

The interplanar distances calculated for all irradiated samples decrease compared to the values obtained for non-irradiated samples. This suggests a tendency towards rearrangement (crystallization) of the polymer into a more compact structure with a smaller interplanar distance.

Table 4.4. Interplanar distances calculated for the samples non-heated / heated and gamma-irradiated.

Irradiated samples	2θ (°)	d(Å)
PSI	19°	4.66 Å
PSI 140 °C	19.3°	4.59 Å
PSI 200 °C	19.3°	4.59 Å
PSI 250 °C	19.3°	4.59 Å
PSI 300 °C	19.3°	4.59 Å
PSI 350 °C	19.3°	4.59 Å

From the comparison of the results in Tables 4.3 and 4.4., it is observed that after the heat treatment, the interplanar distances decrease compared to the initial value of the unheated polystyrene sample, and if we apply in addition to the heat treatment and irradiation of the samples, then the effect becomes more pronounced and the interplanar distance decreases. There are two trends: the first is the arrangement of polymer chains in ordered structures facilitated by the increase of local dynamics with temperature, and, on the other hand, a tendency to disengage

polymer chains from these ordered structures causing this increase in local dynamics. Between the ambient temperature and 200 °C the first process is facilitated, and over 200 °C the second.

In conclusion, it can be stated that gamma irradiation could produce on the one hand, the breaking of polymer chains followed by an ordering process in structures with different diffraction planes compared to the non-irradiated sample, and on the other hand, as in the case of non-irradiated samples, irradiation induces a process of destruction of polymer chains at high temperatures.

4.4. FT-IR analysis

FT-IR spectroscopy analysis of the heated polystyrene samples confirmed once again that heat treatments can cause changes in the structure of the material. The IR spectra obtained for polystyrene samples heated, were compared with the IR spectrum of the unheated sample (PS) and are shown in Figure 4.6.

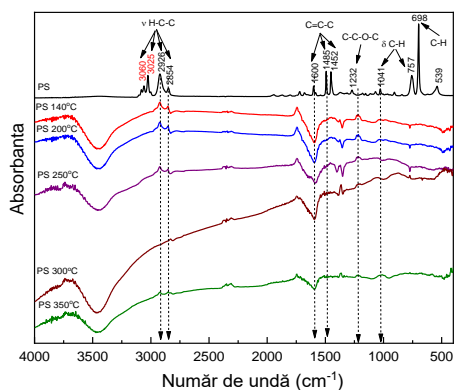


Figure 4.6. FT-IR spectra for initially unheated polystyrene (PS) and for the polystyrene samples heated at temperatures between 140 - 350 °C.

The spectrum of the untreated sample (PS) shows narrow and well-defined vibration bands. The main vibration bands appear at the wave numbers of $\sim 1041 \text{ cm}^{-1}$, 1485 cm^{-1} , 1600 cm^{-1} , 2854 cm^{-1} and 2926 cm^{-1} , respectively. These spectral bands are associated as follows:

- in the spectral range $3000 - 2800 \text{ cm}^{-1}$ the spectral bands from 2926 and 2854 cm^{-1} are associated with the stretching vibrations of the aromatic group H-C-H
- between $1700-1400 \text{ cm}^{-1}$, three absorption bands are identified at 1600 cm^{-1} , 1485 and 1452 cm^{-1} , due to the tensile vibration of the $\text{C} = \text{C} - \text{C}$ group in the phenyl ring
- the low intensity band from 1485 cm^{-1} corresponds to the bending vibration C –H
- the two absorption bands located at 1322 cm^{-1} and at 1041 cm^{-1} are attributed to the tensile vibration C - C - O - C - C, respectively to the bending vibration C - H in the plane of the phenyl group. [40- 42]
- in the low frequency region, two absorption bands are observed and located at 757 and 698 cm^{-1} , which appear most likely due to the C-H vibration out of the plane, indicating a single substituent in the benzene ring. [43]

After polystyrene samples are heated, certain changes appear in the IR spectrum, such as: the disappearance of certain vibration bands, their enlargements, or changes in their amplitude.

For example, in the spectrum of the PS 140 °C sample, the bands of 3060 and 3025 cm⁻¹ disappear, and the bands of 2926 and 2854 cm⁻¹ reduce their amplitude.

Major changes occur in the spectral region 1800–400 cm⁻¹, where vibrations from 757, 698, and 539 cm⁻¹ in the spectrum of the unheated heat (PS) sample are not found in the spectrum of the sample heated to 140 °C. This suggests a significant reduction of molecular vibrations or even their disappearance at these frequencies, caused by the change in the local vicinity of the monomers following the structural reorganization caused by temperature.

At 200 °C and 250 °C, the polystyrene has a behavior almost identical to that treated at 140 °C, suggesting that the vibrational changes caused by heating the samples between 20 °C and 140 °C are maintained in the temperature range of 150 °C - 200 °C.

In the spectrum of the sample heated to 250 °C, the bands from 1232 and 1041 cm⁻¹ disappear, and the others reduce their amplitude.

In the spectrum of the sample heated at 300 °C, it is observed that the bands from 2926 and 2854 cm⁻¹ also disappear, indicating major changes in the molecular vibrations. This is in line with XRD's observations, which in turn indicate important structural changes.

In the spectrum of the sample PS 350 °C, almost all the bands present in the spectrum of the unheated PS sample disappear or significantly reduce their amplitude. In fact, the polymer sample treated at this temperature is almost completely destroyed by the oxidation (combustion) reaction.

The low bandwidth in the low frequency region, observed at 1250 cm⁻¹ is in agreement with other works reported in the literature. [44] The FT-IR results are in agreement with the results of the XRD measurements, which indicate structural changes at high temperatures due to the oxidation and decomposition processes of the material.

4.5. UV-VIS analysis and Fluorescence

Generally, any heat treatment applied to a substance causes changes in color and optical properties, such as light absorption or transparency. These effects were also observed in the studied samples, the reason for which they were investigated by UV-VIS and fluorescence methods. Based on UV-VIS measurements on the unheated polystyrene sample from set 1 (PS) (Fig. 4.7.) it has been established that strong absorption takes place in the vicinity of 300 nm, a wavelength of excitation radiation suitable for fluorescence spectroscopy. Considering this aspect, the fluorescence spectra were recorded for the unheated polystyrene sample, using excitation radiation with three wavelengths, namely: 315 nm, 340 nm and 365 nm respectively. (Fig. 4.8.) From the analysis of the spectra, a large amplitude is observed in the spectral range 340 - 365 nm, and the maximum position of the fluorescence peaks remains unchanged even if the excitation changes, resulting in accordance with the theory. [30, 33]

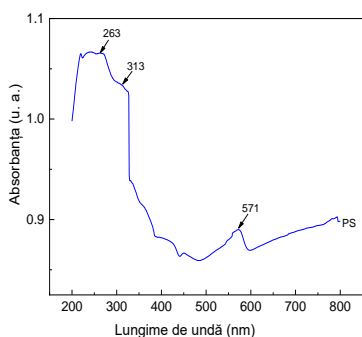


Figure 4.7. UV-VIS absorption spectrum of unheated commercial polystyrene (PS).

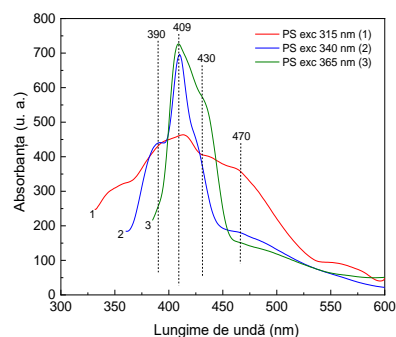


Figure 4.8. Fluorescence spectra of polystyrene PS, excited at 315, 340 and 365 nm.

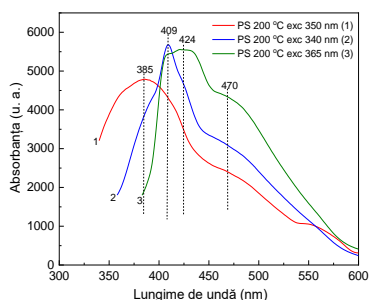


Figure 4.9. Fluorescence spectra of polystyrene heated to 200 °C and excited at 315, 340 and 365 nm.

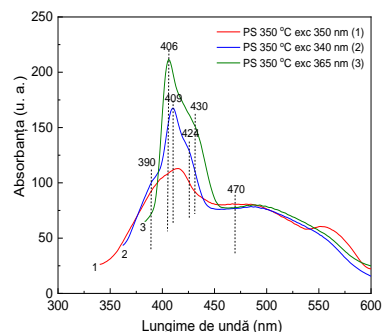


Figure 4.10. Fluorescence spectra of polystyrene samples, heated to 350 °C and excited at 315, 340 and 365 nm.

The fluorescence spectra of the polystyrene samples heated to 200 °C (from set 2), excited at 315 nm, 340 nm and 365 nm showed the appearance of changes after heating in the shape and amplitude of the signal (Fig. 4.9.) The amplitude of all maxima increases in comparison to the amplitude of the signals corresponding to the unheated sample. However, the position of the peaks, given the effect of the overlap, remains unchanged after heating, which shows that the transitions between the electronic levels involved are not affected by the heating process. Increasing the heating temperature of the samples causes a change in the overall shape of the fluorescence spectrum, but the position of the maximum fluorescence remains at 409 nm. This behavior suggests that heat treatment does not induce major changes in e-energy levels. The decrease in amplitude with the increase of the heat treatment temperature is associated with the irreversible degradation of the sample by oxidation. From the analysis of the evolution of fluorescence signals as a function of excitation, the fluorescence effect can be considered the most efficient fluorescence effect obtained at an excitation of 340 nm.

The spectra of the polystyrene samples heated to 350 °C are similar to the spectra of the samples not heated and heated to 200 °C, but the amplitude of the peaks is greatly reduced. (Fig. 4.10.) All excitations are followed by a fluorescence emission centered between 406 nm and 409 nm. The shape of the signal is determined by the different contributions of the transitions between states S1 and S0 to the fluorescence effect when the excitation frequency

changes. The overlap of the signals associated with these transitions gives rise to a resulting wider fluorescence spectrum. Increasing the heating temperature of the samples causes a change in the overall shape of the fluorescence spectrum, but the position of the maximum fluorescence remains at 409 nm. This behavior suggests that heat treatment does not induce major changes in e-energy levels. The decrease in amplitude with the increase of the heat treatment temperature is associated with the irreversible degradation of the sample by oxidation. From the analysis of the evolution of fluorescence signals as a function of excitation, the fluorescence effect can be considered the most efficient fluorescence effect obtained at an excitation of 340 nm.

4.6. Conclusions.

The results obtained after investigations of the polystyrene samples by XRD, FT-IR, UV-VIS, and fluorescence show that certain structural changes appeared, which are related to the arrangement of polymer chains.

XRD analysis has shown that heating the polystyrene to 200 °C leads to a local arrangement of the polymer chains in ordered structures. The slight displacement of the diffraction maximum from $2\theta = 17.8^\circ$ in the unheated sample to $2\theta = 18.7^\circ$ in the sample heated to 200 °C indicated the evolution of the polymer matrix towards a more compact structure. This ordering process is mainly in the temperature range 20 - 200 °C, when an increase in the intensity of diffraction peaks is observed. Above this temperature their intensity decreases, which indicates the destruction of the ordered phase. This effect is determined by the amplitude of the dynamics of the polymer chains as the thermal agitation increases. At the same time, the process of oxidation and destruction by combustion of the polymer structure appears here.

From the FT-IR spectra of the polystyrene samples it was found that there are differences between the heated and unheated samples, both by the disappearance of the C-H vibration bands from 3060, 3025, 757, 698 and 539 cm^{-1} , and by the decrease of the vibration intensity from 2926, 2854 and 1486 cm^{-1} . In the case of irradiated samples, we also observe an ordering tendency up to temperatures of a maximum of 200 °C. The intensity of the diffraction peaks increases and we even signal the appearance of new peaks at $2\theta = 29^\circ$ and 42° , interaction with gamma radiation. The new peaks indicate ordered structures with smaller interplanetary distances, most likely determined by the rearrangement of shorter polymer chains, determined by the interaction with gamma radiation. At a given temperature, short chains have higher mobility than long chains, which allows them to be more easily arranged in orderly structures. But increasing thermal agitation with increasing temperature also has a destructive effect on these ordered areas. This is demonstrated by the decrease in the intensity of all diffraction peaks, including new ones at $2\theta = 29^\circ$ and 42° , above temperatures of 250 °C. We have two competing processes, on the one hand a tendency of ordering caused by a greater dynamics of the polymer chains and, on the other hand, a tendency of destruction of these structures determined by the increase of the thermal agitation. But overall, the difference between the diffractograms of the irradiated and non-irradiated samples shows a clear effect of gamma irradiation on the polymer structure.

Based on the UV-VIS absorption spectra obtained on thermally degraded polystyrene samples, it was established that the most efficient fluorescence excitation wavelengths are 315 nm, 340 nm and 365 nm. The spectra of the excited samples at different wavelengths contain signals with widths and amplitudes depending on the frequency of

excitation, behavior correlated with the probabilities of transition between the electronic levels involved in fluorescence emission. The most important peak occurs at 409 nm regardless of the excitation frequency, but its amplitude depends on the excitation. Given the amplitude and width of this fluorescence peak, we consider 340 nm to be the most efficient excitation radiation. After heat treatment the position of the maximums of the fluorescence curves remains unchanged, but their amplitude and width depend on the temperature. At 200 °C the general appearance of the spectra is similar to that obtained for the unheated sample, whereas at 350 °C the amplitude of the peaks decreases dramatically due to the oxidation process of a part of the sample. However, the stable position of the fluorescence maxima suggests good stability of polystyrene even at high temperatures. This property can be taken into account in the technological processes of recycling these materials by heat treatment.

Chapter 5: Experimental results - PET

The aim of this study was to highlight the structural changes that occur in PET polyethylene terephthalate samples as a result of thermal degradation and gamma irradiation. For this purpose, degraded samples were analyzed by applying a heat treatment of progressive heating up to 300 °C, followed by a slow cooling by passive convection at ambient temperature, and thermally degraded samples were then exposed to gamma radiation. All samples were analyzed by complementary methods: X-ray diffraction, TG analysis and infrared spectroscopy (FT-IR).

5.1. XRD analysis

XRD measurements were performed on the following samples: **G00 initially**, **G00 melted-cooled**, **G01 irradiated 456 Gy**, **G02 irradiated 3 kGy**, **G03 irradiated 7 kGy**, **G01 melted-cooled 456 Gy**, **G02 melted-cooled 3 kGy**, and **G03 melted-cooled 7 kGy** respectively.

5.1.1. Analysis of thermally degraded commercial PET samples by melting followed by cooling

The diffractograms obtained on the commercial PET sample (G00 initially) and on the heat-treated sample (G00 melted-cooled) are presented in Figure 5.1.

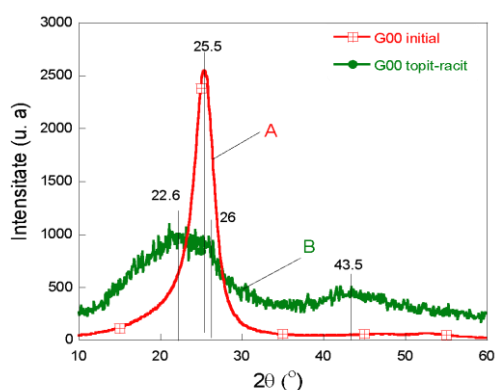


Figure 5.1. XRD diffractograms for the PET sample before heat treatment (initial G00, curve A) and after melting-cooling (melted-cooled G00, curve B).

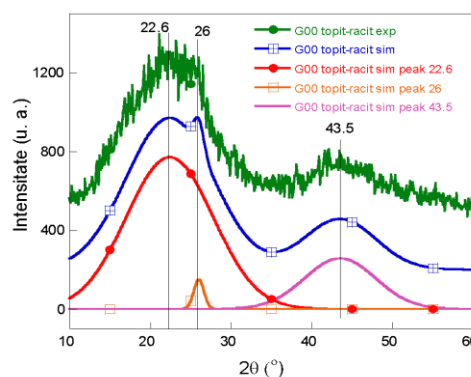


Figure 5.2. Experimental diffractogram of PET sample after heat treatment (melted-cooled G00) compared with simulated diffractograms at diffraction angles 22.6, 26 and 43.5°.

Table 5.1. Calculation of interplanar distances for G00 and G00 melted-cooled.

Non-irradiated samples	2θ (°)	d(Å)	Structure
G00	25.5°	3.48 Å	amorphous+crystalline
G00 melted-cooled	22.6°	3.93 Å	amorphous
	26°	3.42 Å	amorphous
	43.5°	2.07 Å	amorphous

It can be observed that the diffractogram of the initial G00 sample presents both amorphous and crystalline phases, a structure with local order due to the parallel arrangement of some portions of the polymer chains. [22] (Fig.5.1, curve A). [22] (Fig.5.1, curve A).

By applying the Bragg equation for the maximum diffraction line from $2\theta = 25.5^\circ$, the interplanar distance between two polymer chains was calculated and the value $d = 3.48 \text{ \AA}$ was obtained. This shows that the sample G00 initially contains several ordered domains. Apart from these crystalline domains, the polymer chains are in the amorphous phase which leads to the widening of the diffraction spectrum. From the analysis of the diffractogram of the G00 heat-melted-cooled PET sample, it is observed that there are changes in the amplitude and position of the diffraction line. (Fig. 5.1. Curve B) By heating process applied to PET, polymer chains tend to decouple from the ordered arrangement by diffusion or repetition, [1, 45] in the samples new ordered fields appear, and the crystallographic planes will have different interplanar distances. Thus, the intense peak from 25.5° in G00 initially is replaced in the diffractogram of the G00 melt-cooled heat-treated sample by three peaks of lower intensity, with maxima at diffraction angles $2\theta = 22.6^\circ$, 26° and 43.5° . The maximum of the diffraction line from $2\theta = 26^\circ$ in the diffractogram of the G00 melt-cooled sample corresponds to the peak from $2\theta = 25.5^\circ$ in the diffractogram of the unheated sample (G00 initial). On the other hand, the intensity of the peaks in the diffractogram of the heat-treated sample is much reduced and there is a shift of the maximums of the peaks to larger angles. There is a reduction of the ordered phase fraction from the G00 initial sample (which was $2\theta = 25.5^\circ$) and a decrease in the interplanar distance in the molten and cooled sample (G00 melted-cooled) from the value $d = 3.48 \text{ \AA}$ -in the untreated sample at $d = 3.42 \text{ \AA}$. This new ordered phase is more compact, and the new wide peaks from $2\theta = 22.6^\circ$ and 43.5° indicate the appearance of new ordered domains, with different interplanar distances, namely $d = 3.93 \text{ \AA}$ (at the phase corresponding to the peak from 22.6°) and respectively $d = 2.07 \text{ \AA}$ (at the phase corresponding to the peak at 43.5°).

By simulating the diffractograms with the Gauss function (Chapter 3. Ec. 4) for the diffraction angles of 22.6° , 26° , and 43.5° , the parameters presented in Table 5.1 were obtained.

Compared to the diffractogram of the initial G00 sample, it can also be seen that the crystalline phase corresponding to the peak of $2\theta = 26^\circ$, represents only 1.8% of the entire phase. There is massive destruction of the crystalline phase after the thermal process of melting and cooling, and the new maximum from $2\theta = 22.6^\circ$ is very wide, its area representing 77% of the entire XRD spectrum, which means that there is a massive increase of amorphous phase to the detriment of the initial crystalline phase. Heating allows the polymer chains to leave the ordered structure and adopt a disordered arrangement.

The peak at 43.5° is associated with the appearance of a new ordered local structure with a small interplanar distance, $d = 2.07 \text{ \AA}$. This effect is determined by the association in small locally ordered domains of the shorter chains resulting from a process of breaking them.

Table 5.2. G00 Melt-cooled heat-treated sample diffractogram simulation parameters.

2 θ [degrees]	S [u. a.]	S/S _{tot} [%]	d [Å]
22.6	10283	77	3.96
26	234	1.8	3.42
43.5	2844	21.2	2.07

S = area under each peak, S_{tot} = 3635 u.a. is the area of the whole spectrum, d = the interplanar distance corresponding to the diffraction maxima, S / S_{tot} = the crystalline phase fraction corresponding to each peak in the whole PET sample.

The diffractogram of the heat-treated sample (G00 melted-cooled), contains peaks with a low intensity compared to the peaks in the commercial sample (G00 initial), which highlights a decrease in crystallinity of the material following the application of heat treatment. By melting PET materials, there is a massive destruction of the initial crystalline phase and the emergence of new crystallization centers with greater interplanar distance, and an increase in the share of the amorphous phase in polymers.

5.1.2. Analysis of gamma-irradiated PET samples.

5.1.2.1. Analysis of commercial gamma-irradiated PET samples.

By comparing the diffractograms obtained for the untreated G00 initially, with the diffractograms corresponding to the samples which absorbed the three radiation doses (G01 irradiated 456 Gy, G02 irradiated 3 kGy and G03 irradiated 7 kGy), it is found that they are very similar. (Fig. 5.3.) Only a slight change in the amplitude of diffraction peaks is observed for radiation doses above 1 kGy.

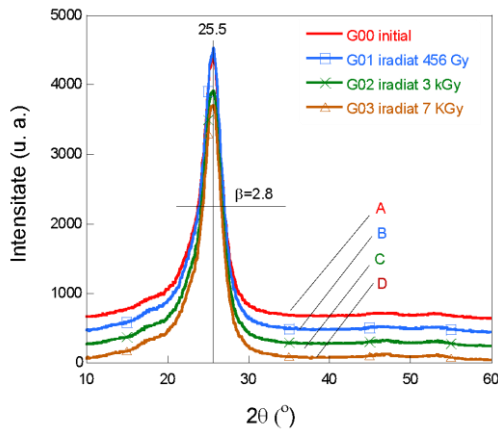


Figure 5.3. Diffractograms of non-heat treated PET samples after gamma-irradiation: G00 initially (curve A), G01 irradiated 456 Gy (curve B), G02 irradiated 3 kGy (curve C) and G03 irradiated 7 kGy (curve D).

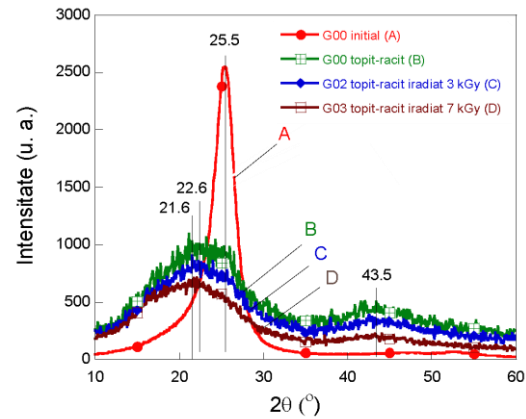


Figure 5.4. XRD diffractograms for PET samples: unirradiated G00 initially (curve A), heat-treated melted-cooled G00 (curve B), and heat-treated with gamma-irradiation - G02 melted-cooled irradiated 3 kGy (curve C) and at 7 kGy - G03 melted-cooled irradiated 7 kGy (curve D).

The intense and narrow peak at the angle $2\theta = 25.5^\circ$ is present in all three diffractograms of gamma-irradiated PET samples and corresponds to an interplanar distance $d = 3.48 \text{ \AA}$.

The value of the half-height $\beta = 2.8^\circ$ is the same for all samples, this indicating a dispersion of interplanar distances between 3.72 and 3.35 \AA , as in the case of the initially non-irradiated G00 sample. These results show that gamma irradiation of PET between $465 \text{ Gy} - 7 \text{ kGy}$ can only produce a cleavage of polymer chains with a disordered arrangement of polymer chains. [45, 46]

5.1.2.2. Analysis of thermally degraded PET samples by heating-cooling, and then gamma-irradiated

The diffractograms of the treated and then irradiated samples were marked with G01 molten-cooled irradiated 456 Gy , G02 molten-cooled irradiated 3 kGy and G03 molten-cooled irradiated 7 kGy . The diffractogram of sample G01 melted-cooled irradiated 456 Gy is almost similar to that of the heat-treated but non-irradiated sample (G00 melted-cooled). For this reason it was not included in comparison with the diffractograms obtained on samples treated and irradiated at 3 and 7 kGy , presented in Figure 5.4.

The diffractograms of the heat-treated and then irradiated samples show significant changes compared to the initial G00 sample. Associated with the heating effect, the irradiation process leads to faster destruction of the ordered phase, an additional modification of the XRD model of the heated and irradiated samples occurs, and the effect increases with the absorbed radiation dose.

After irradiation of the heat-treated samples, the maximum peak from 25.5° in G00, becomes much wider and decreases in amplitude in the diffractograms of the heat-treated and then irradiated samples. There is also a slight shift of the maximum peak from 25.5° (in G00 initial) to lower diffraction angles, to 22.6° and 21.6° after heat treatment and irradiation. These changes are more evident in the heat-treated samples with radiation doses of 3 and 7 kGy . As the irradiation dose increases, the angle at which the maximum diffraction occurs decreases, and the peak at 43.5° decreases in intensity.

From the comparison of the diffractograms of the heat-treated samples and then irradiated (G00 melted-cooled irradiated) with the G00 initial sample (Fig. 5. 4.), it is observed that the chain splitting effect is more pronounced in the treated and irradiated samples, allowing the chains to decouple easily and adopt a messy arrangement. Associated with the heating effect, this irradiation process leads to faster destruction of the ordered phase and the increase of the amorphous phase weight, Figure 5.5., and this effect increases with the increase of the absorbed radiation dose.

Quantitative analysis of diffractograms corresponding to the samples G02 melted-cooled irradiated 3 kGy and G03 melted-cooled irradiated 7 kGy , was performed by simulation previously applied for non-irradiated samples.

The simulated diffractograms (Figure 5.6) and the parameters of diffractogram simulation are presented in Table 5.2.

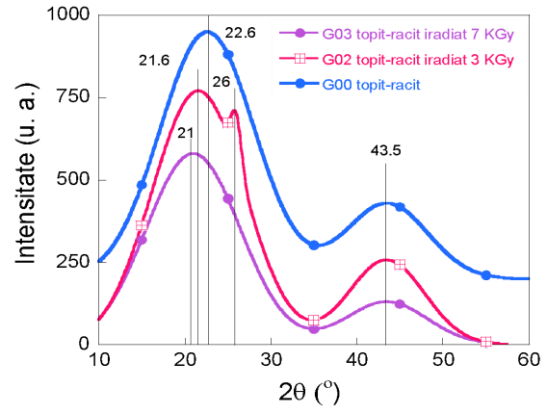


Figure 5.5. XRD diffractograms for non-irradiated molten-cooled PET sample (G00 melted-cooled), heat-treated and gamma irradiated PET samples G02 melted-cooled irradiated 3 kGy and G03 melted-cooled irradiated 7 kGy.

The analysis of the diffractograms shows that there is an enlargement of the diffraction line by overlapping the peak from $2\theta = 26^\circ$ with a new peak located at 21.6° , with an interplanar distance $d = 4.11 \text{ \AA}$. Therefore, in the sample appears a new ordered phase with the interplanar distance $d = 4.11 \text{ \AA}$ (at $2\theta = 21.6^\circ$) that coexists together with the initial phase with $d = 3.42 \text{ \AA}$ which corresponds to the peak from $2\theta = 26^\circ$. Also an ordered structure can be observed in the simulation which has the interplanar distance of $d = 2.07 \text{ \AA}$ corresponding to the peak $2\theta = 43.5^\circ$. The percent of these phases is given by the ratio between the area of each peak and the area of the whole spectrum and is presented in Table 5.3.

Table 5.3. Parameters of the simulated diffractogram of the sample G02 melted-cooled irradiated 3 kGy.

2θ [degrees]	S [u. a.]	S/S_{tot} [%]	d [Å]
21.6	7580	80	4.11
26	158	1.7	3.42
43.5	1660	18.3	2.07

At the same time, the fraction of this phase increases from 77% for the non-irradiated sample (G00 melted-cooled) (Table 5.2.) to 80% for the G02 melted-cooled irradiated 3 kGy sample. (Table 5.3.) The peaks at 26° and 43.5° remain unchanged, but the area delimited by them decreases due to the reduction of the ordered phase fraction.

The results of this study lead to the conclusion that thermal degradation is more pronounced for irradiated samples than for non-irradiated samples. This result is also confirmed by the behavior of the G03 sample irradiated with 7 kGy.

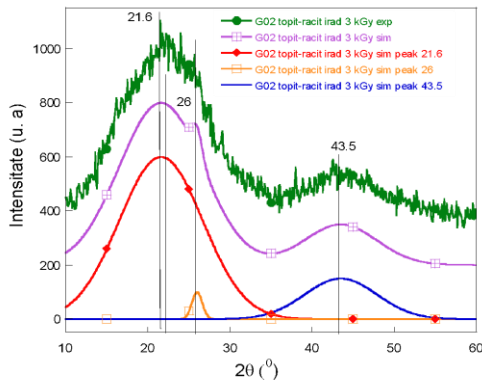


Figure 5.6. The simulated diffractograms of the G02 melted-cooled irradiated 3 kGy sample.

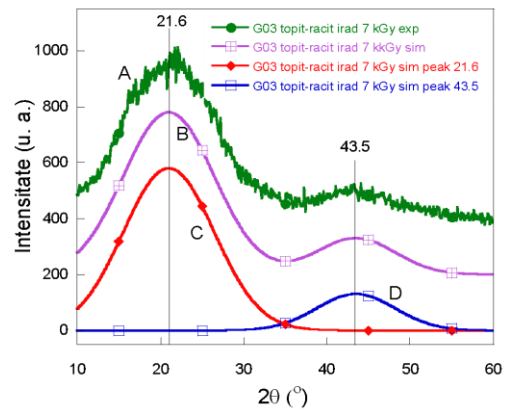


Figure 5.7. The simulated diffractograms of the G03 melted-cooled irradiated 7 kGy sample.

From the analysis of the simulated diffractograms for the G03 melted-cooled irradiated 7 kGy sample., presented in Figure 5.6., a decrease in the amplitude of all diffraction maxima is observed and the peak from 26° disappears. This result indicates the complete destruction of the ordered phase - observed in the samples before heating, only the peaks at 21.6° and 43.5° are preserved.

The simulation parameters of G03 molten-cooled irradiated 7 kGy sample diffractograms are presented in Table 5.3. The fraction of the amorphous phase due to the first peak increases to 83.4%, while the fraction of the phase due to the second peak decreases to 16.6%.

Table 5.4. Parameters of the simulated diffractogram of the sample G03 melted-cooled irradiated 7 kGy.

2θ [degrees]	S [u. a.]	S/S_{tot} [%]	d [Å]
21.6	7785	83.4	4.11
43.5	1545	16.6	2.07

From the presented analysis, we have the following conclusions:

- By irradiating the PET materials, there is a displacement of the maximum diffraction line from 22.6° in the non-irradiated sample (G00 melted-cooled), to 21.6° in the treated and irradiated sample at 3 kGy and respectively at 21° in the treated and irradiated sample the 7 kGy.
- There is also an evolution of the S / Stot peak area from 77% (Tab. 5.1.) in the non-irradiated sample (G00 melted-cooled) to 80% (Tab. 5.2.) in the treated and irradiated sample at 3 kGy (G02 melted-cooled irradiated 3 kGy), reaching 83% (Tab. 5.3.) in the irradiated sample at 7 kGy (G03 molten-cooled).

5.2. DTA analysis

DTA / TGA thermal analysis on the samples non-irradiated and irradiated are presented in Figure 5.8. DTA curve obtained for the initial G00 sample shows a first broad endothermic signal with a maximum at about 150 °C highlighting the crystallization process, an event also explained with XRD. The second endothermic signal observed at ~ 252 °C corresponds to the beginning of the thermal decomposition of the sample, a result which is also in agreement with the XRD observations, which indicate structural changes at temperatures higher than 200 °C.

The sample G00 melted-cooled irradiated 7 kGy (curve B) exhibits a behavior similar to that of the non-irradiated sample, with the difference that the endothermic signal in the temperature range 80 - 200 °C is wider. The irradiated sample also contains broken chains due to absorption, has a higher dispersion of ordered fields, compared to the non-irradiated sample, with polymer chains of different lengths, which can be organized in ordered structures with distances between different chains, so in a more great diversity of crystalline structures.

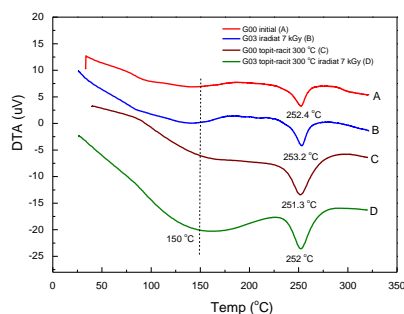


Figure 5.8. DTA curves for G00 initial (curve A), G03 irradiated 7 kGy, (curve B), G00 melted-cooled (curve C), and G03 melted-cooled irradiated 7 kGy (curve D).

For the heat-treated sample which absorbed the 7 kGy radiation (curve D), due to the high absorption of gamma photons, the share of polymer chain breakage events is higher than the non-irradiated or irradiated samples with low doses. We have a greater dispersion of the length of the polymer chains, with different dynamics, which favors the organization in several ordered structures, with different arrangement characteristics each with its own thermal behavior. Their overlap determines the accentuated widening of the endothermic signal in the temperature range of 80 - 200 °C, with the maximum at approximately 150 °C. On the other hand, a strong endothermic signal is observed at 252 °C regardless of the degree of irradiation. We assume that it is associated with the decomposition of samples, a phenomenon that does not depend on the length of the polymer chains but only on their molecular structure. The latter is slightly affected by irradiation, which is why all samples, regardless of irradiation, behave the same way (the structure of the monomer is the same in all samples). The length of the polymer chains does not influence this phenomenon.

5.3. Conclusions

The complementary methods XRD and DTA / DTG, provided information related to the local organization of the polymer chains, their structure at the level of molecular vibrations, but also to their thermal behavior.

- PET samples in an initial-undegraded state, without heat or radiative treatment, have a semicrystalline character with an important amorphous phase, associated with the maximum diffraction from $2\theta = 25.5^\circ$.
- The heat treatment modifies the dynamics of the polymer chains and their rearrangement into ordered structures, a process identified by the appearance of new diffraction peaks and by the modification of the characteristics of the initial signal. For non-irradiated samples, we notice an ordering trend in the temperature range of 20 - 200 °C. Above 200 °C, although the ordering trend persists, the process of destroying the ordered structures becomes predominant, a phenomenon indicated by the decrease of the amplitude of the diffraction peaks.
- The presented results show that the structural changes are different in the heat-treated and then irradiated samples, compared to the behavior of the non-heat-treated and irradiated samples. The heat treatment together with the irradiation of the PET samples lead to the destruction of the initial ordered structure of the PET materials and show, at the same time, that this effect is dependent on the radiation dose.

Chapter 6: Experimental results - FS and FD

Teeth are a component of the human body, being subjected to continuous degradation. For this purpose, samples from human teeth were analyzed by X-ray diffraction and infrared spectroscopy (FT-IR), in several stages:

- ✓ in the initial state-without degradation,
- ✓ after a chemical degradation in citric acid 4 to 8 days and,
- ✓ after a period of relaxation of the tooth outside the degrading agent.

6.1. XRD analysis

X-ray diffractograms obtained for the initial enamel sample (FS) and the sample immersed for 4 days in citric acid (FS-4dCI) were compared with the diffractograms of the citric acid (CI) and of the hydroxyapatite (HA). (Fig. 6.1)

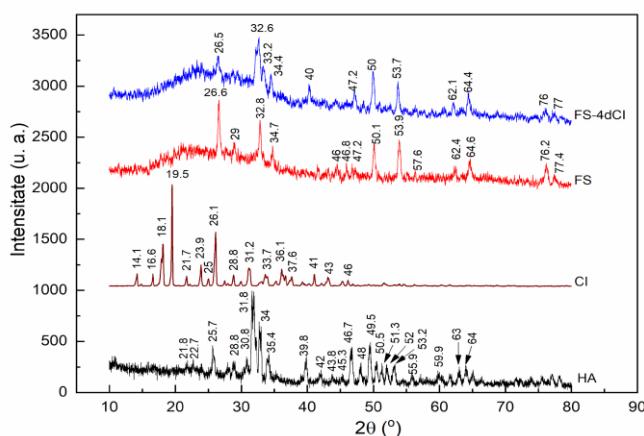


Figura 6.1. XRD diffractograms for HA, CI, enamel sample before immersion in citric acid (FS), and enamel sample after 4 days of immersion in citric acid (FS-4dCI).

The diffractogram of the enamel sample (FS) before immersion in citric acid, contains in the angular range $2\theta = 10 - 40^\circ$ a wide diffraction line determined by the non-crystalline part of the hydroxyapatite. [47] Over this amorphous region overlap several diffraction lines with maxima at $2\theta = 26.6^\circ, 32.8^\circ, 34.7^\circ$. Each diffraction line was assigned Miller indices corresponding to the crystallographic planes by identification with the PDF file in the database provided by the International Center for Diffraction Data JCPDS. Thus, for the crystalline portion of the hydroxyapatite diffractogram, the crystallographic planes (002), (211) and (300) were identified according to PDF 024-0033 and PDF 86-1200. [49] At $2\theta = 50.1^\circ$ and 53.9° the diffraction lines assigned to the hydroxyapatite planes (213) and (004) were identified. [11]

The diffractogram of the FS-4dCI sample after four days of immersion in citric acid is very similar to that obtained for the same sample before immersion (FS sample). The diffraction lines are found at the same values as the initial sample, and their intensities are similar. The only exceptions are the lines with maxima at $2\theta = 26.5^\circ$ and 47.2° which have lower intensities. In this diffractogram appear two new diffraction lines, the first with the maximum at $2\theta = 40^\circ$ corresponding to the presence of hydroxyapatite, (in HA at 39.8°) and the second line with the maximum at $2\theta = 26.5^\circ$ which was associated with citric acid (in CI was the 26.1°). Apart from these lines, no other new

diffraction lines are identified due to the presence of citric acid, which proves that the enamel has a very good stability in case of exposure to citric acid for a moderate period of time and does not allow penetration of acid in the enamel structure.

Enamel samples immersed in citric acid for 4 days and left for 30 days in the dark, outside the action of citric acid, (FS-4dCI + 30dRT) were analyzed by XRD in order to identify certain structural changes in time. (Fig. 6.2.) Comparing the diffraction pattern of the enamel sample immediately after degradation to citric acid (FS-4dCI) with the diffractogram of the same sample after 30 days of storage (FS-4dCI + 30dRT), it is observed that the main diffraction lines corresponding to the FS-4dCI sample appear at the same diffraction angle and with a similar amplitude in the case of the sample FS-4dCI + 30dRT.

To verify that the sampling time in the citric acid solution influences the structure of the teeth, one of the samples with the enamel (FS) was left in the citric acid solution for up to 8 days (FS-8dCI), after which they were measured by XRD. The obtained diffractogram was compared with the diffractograms of the sample in the initial state (FS), respectively with the diffractogram of the sample immersed for 4 days in the citric acid solution (FS-8dCI). (Fig. 6.3

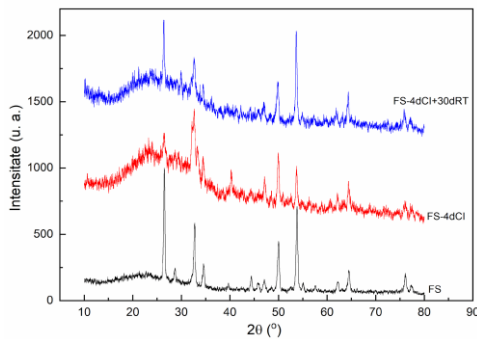


Figure 6.2. XRD diffractograms for the enamel samples: FS, FS-4dCI and FS-4dCI + 30dRT.

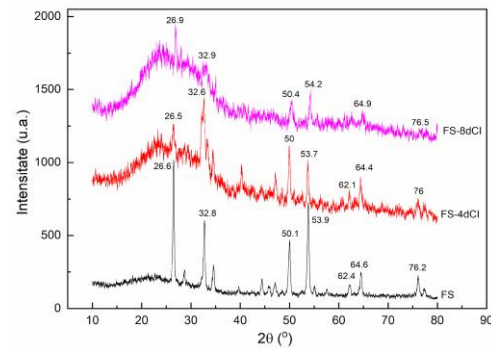


Figure 6.3. XRD diffractograms for enamel samples FS, FS-4dCI and FS-8dCI, respectively

From the XRD analysis of the FS-8dCI sample, it is observed that no major changes occur after eight days of maintaining the citric acid sample, but the diffraction lines of the FS-8dCI sample decrease in intensity compared to those of the enamel sample maintained for only four days in citric acid and the maximums of the diffraction lines are slightly shifted towards higher values, at $2\theta = 26.9^\circ, 32.9^\circ, 50.4^\circ, 54.2^\circ, 64.9^\circ$ and 76.5° respectively

Similar investigations were performed on the initial dentin sample (FD) and on the dentin sample that was immersed in citric acid for four days (FD-4dCI). The XRD diffractograms obtained were compared with those of hydroxyapatite (HA) and citric acid (CI). (Fig. 6.4.) The diffractogram of the initial dentin sample (FD) contains in the angular range 10° and 40° a portion with wider diffraction lines and maximums at $2\theta = 22.7^\circ, 31.8^\circ, 33^\circ, 49.6^\circ, 53.4^\circ$. These angles can also be seen in the diffraction pattern of the enamel veneer, which indicates that they correspond to similar diffraction planes. The values at which some of these diffraction maxima appear are very close to the values corresponding to hydroxyapatite where they appear at $2\theta = 31.8^\circ, 32.8^\circ, 49.5^\circ, 53.2^\circ$.

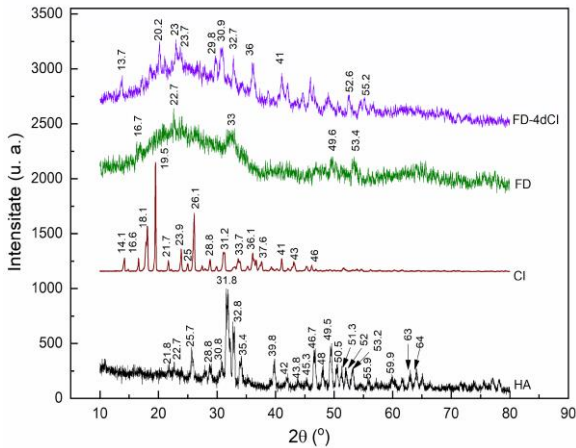


Figure 6.4. XRD diffractograms for the dentine samples: FD, FD-4dCI and FD-4dCI + 30dRT

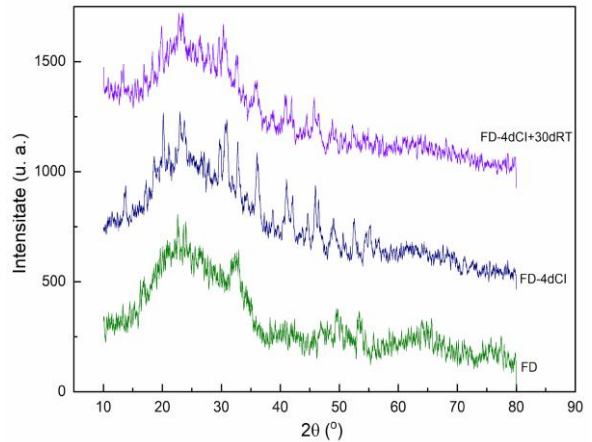


Figure 6.5. XRD diffractograms for the dentine samples: FD, FD-4dCI and FD-4dCI + 30dRT.

This behavior is normal given that hydroxyapatite is the main component of enamel and dentine. However, the maximum diffraction lines of the dentin are wider than those obtained for enamel samples. This is explained by the difference between the crystallite size of enamel ($D_{FS} \sim 50$ nm) which has a higher value than the value of the crystallite size of the dentine ($D_{FD} \sim 10$ nm). [11]

The diffractogram obtained after the immersion of dentine for 4 days in citric acid (FD-4dCI) shows some changes compared to the diffractogram of the initial sample, it contains a portion with wider and maximum diffraction lines located at $2\theta = 13.7^\circ, 20.2^\circ, 23^\circ, 23.7^\circ, 29.8^\circ, 30.9^\circ, 32.7^\circ, 36^\circ, 41^\circ, 42^\circ, 42.2^\circ, 42.2^\circ, 55^\circ$. The diffraction lines with maxima at $2\theta = 23.9^\circ, 31.2^\circ, 36.1^\circ, 41^\circ$ were attributed to the presence of citric acid, these values being very close to the values obtained for pure citric acid. Based on the appearance of these new diffraction lines, it can be stated that without the protection of the enamel, citric acid enters the structure of the dentine. The diffractogram of the FD-4dCI sample contains some lines characteristic of hydroxyapatite located at $2\theta = 30.8^\circ$ and 32.8° , which indicates the persistence of hydroxyapatite in dentine. The absence of certain diffraction lines in the diffractogram of the FD-4dCI sample sustains the partial destruction of dentine by citric acid. One of the samples with dentin immersed in citric acid for 4 days was allowed to relax for 30 days without the action of citric acid (FD-4dCI + 30dRT). The XRD diffractogram obtained for this sample was compared with that of the FD sample before and after immersion in citric acid (FD and FD-4dCI). (Fig. 6.5.) From the comparison of the diffractograms obtained for the initial dentine sample, after immersion in citric acid and after relaxation without the action of citric acid, it is found that the samples show a behavior similar to that of enamel samples that does not change. This result indicates good structural stability for a 30-day period of dentine, which has previously been degraded in citric acid for 4 days.

To verify that the behavior of the dentine is influenced by the duration of immersion of the sample in the citric acid solution, a sample with the dentine was maintained in the citric acid solution for 8 days (FD-8dCI). The diffractogram obtained for (FD-8dCI) was compared with that of the initial sample (FD) and the immersed sample for 4 days (FD-4dCI). (Fig. 6.6)

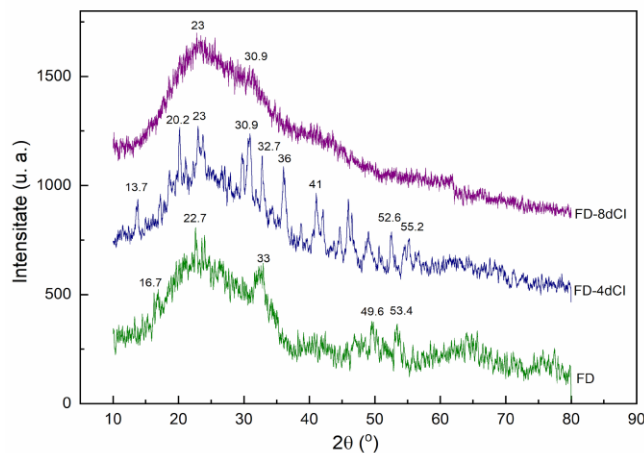


Figure 6.6. XRD diffractograms for dentine samples FD, FD-4dCI and FD-8dCI, respectively

From the comparison of the diffractograms obtained for the sample degraded in citric acid for 8 days (FD-8dCI), it is observed that in the region 2θ : $20 - 35^\circ$ the main diffraction lines keep their maxima at the same value but are wider and the rest of the diffractogram has the tendency of an amorphous structure. The widening of the diffraction lines indicates the destruction of the ordered structure after the action of citric acid for 8 days.

By comparing the XRD results obtained for the enamel and dentine samples immersed for 8 days in citric acid solution, it is found that, as the action time of the citric acid increases, there is massive destruction of the enamel in the case of the FS sample and an amorphization of the structure in the case of the FD sample. What remains after 8 days of immersion in citric acid consists only of dentine in both FS and FD samples.

6.2. FT-IR analysis

Through the FT-IR analysis of the samples with enamel and dentine, the aim was to obtain information on a molecular scale, regarding the possible chemical reaction between citric acid and teeth. Each new component resulting from the chemical reaction will be followed by changes in the vibrational spectrum of the initial samples. The enamel sample (FS) was initially analyzed before chemical degradation by immersion in citric acid (Fig. 6.7).

The FT-IR spectrum of the FS sample contains vibration bands located at $\sim 1632, 1461, 1418, 1035, 604, 564 \text{ cm}^{-1}$ and low intensity peaks - shoulders, at $1095, 957$ and 873 cm^{-1} . In the spectral range $1190-970 \text{ cm}^{-1}$ there are bands due to the phosphate group PO_4^{3-} , with peaks at $1095, 1035$ and 957 cm^{-1} . The carbonate ions CO_3^{2-} occupy two positions [50], in the region $1650-1300 \text{ cm}^{-1}$ three bands are observed at $1551, 1461$ and 1418 cm^{-1} which indicate the inclusion of CO_3^{2-} in the OH^- position [11]. The low frequency band from 873 cm^{-1} is also due to the vibration of the CO_3^{2-} groups. The medium intensity bands from 564 and 604 cm^{-1} are due to the adsorbed water. [49]

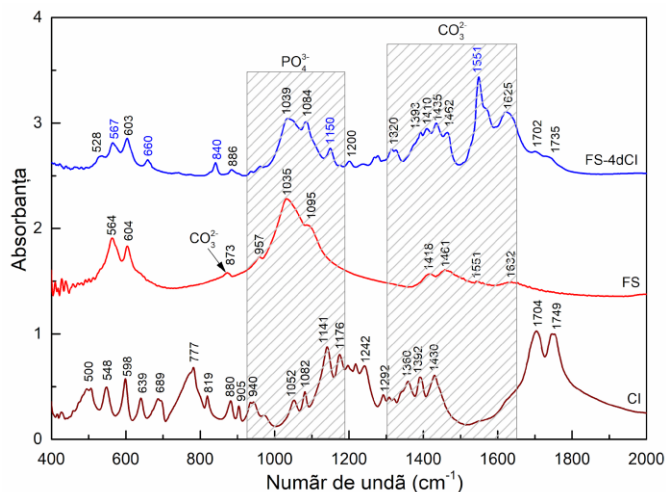


Figure 6.7. FTIR spectra in the range 400 - 2000 cm^{-1} for the initial enamel sample (FS) and after 4 days of immersion in citric acid (FS-4dCI), compared to the citric acid spectrum.

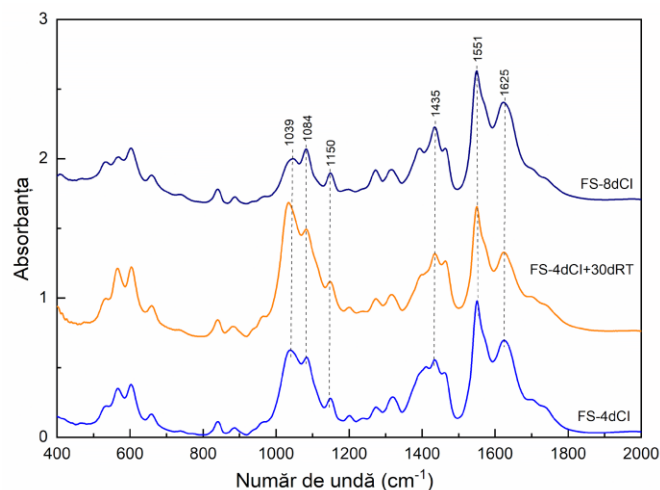


Figure 6.8. FT-IR spectra in the range 400–2000 cm^{-1} of the FS-4dCI sample after 30 days of storage at RT and after 8 days of immersion in citric acid.

Compared to the FT-IR spectrum of the initial sample (FS), after maintaining the enamel sample in the 4-day citric acid solution (FS-4dCI) in the spectrum, some changes are observed due to the interaction of the tooth with citric acid. Thus, the existing vibrations in the initial sample appear in the FS-4dCI spectrum at slightly modified values. There are also new vibration modes at ~ 660 , 840 , 1150 and 1551 cm^{-1} and a shoulder at $\sim 567 \text{ cm}^{-1}$ due to the interaction of the enamel with citric acid. The peak located at $\sim 1632 \text{ cm}^{-1}$ in the FS spectrum, appears displaced at 1625 cm^{-1} in the sample spectrum after immersion, and with higher intensity, this change indicates the increase of the amount of water in the tooth after immersion in citric acid. The vibrations of the phosphate group PO_4^{3-} also appear in the spectrum of the sample FS-4dCI at slightly displaced values, at 1084 and 1393 cm^{-1} , these displacements being the effect of the interaction of the enamel with the citric acid. The vibrations characteristic of citric acid (CI) appear in the spectrum of the immersed sample slightly displaced from 1082 cm^{-1} (in the spectrum at CI) to 1084 cm^{-1} (in FS-4dCI). Also due to the presence of citric acid, new vibrations appear in the spectrum of the immersed sample at 1702 and 1735 cm^{-1} in the form of low intensity shoulders. The appearance of new vibrations is explained by the penetration of citric acid in the enamel structure, this result being in accordance with the XRD results. The FT-IR spectrum of the sample relaxed for 30 days FS-4dCI + 30dRT shown in Figure 6.8, shows no changes compared to the spectrum of the sample immersed 4 days in citric acid, which means that the enamel has a good stability after this storage period for 30 days. The spectrum of the FS sample immersed in citric acid for 8 days looks almost similar to the spectrum of the sample before storage for 30 days, with the difference that the amplitude of the bands from 1039 and 1084 cm^{-1} decreases. The other vibrations from 1150 , 1435 , 1551 and 1625 cm^{-1} remain unchanged, which confirms good chemical stability of the enamel against citric acid.

Similar investigations were performed on the dentine sample (FD) before and after the 4-day immersion sample in citric acid (FD-4dCI). (Fig. 6.9) The FT-IR spectrum of the initial sample with dentine (FD), contains characteristic vibration bands located at ~ 1663 , 1546 , 1455 , 1418 , 1031 , 872 , 604 , 561 cm^{-1} and shoulders at 1095 and 957 cm^{-1} .

In the spectrum of FD sample, the bands from 1095, 1031 and 957 cm^{-1} due to the PO_4^{3-} group, appear slightly displaced compared to the values at which they appear in the spectrum of the FS sample, this is most likely due to the crystallinity differences between enamel and dentine. [52, 53] The vibration of hydroxyapatite CO_3^{2-} located at 1551 cm^{-1} in the enamel spectrum, in the dentine spectrum are shifted to $\sim 1546 \text{ cm}^{-1}$, and the medium intensity bands due to the adsorbed water are found at 561 and 604 cm^{-1} . After immersing the dentine sample in the citric acid solution, in the spectrum of FD-4dCI, the vibration of the CO_3^{2-} carbon groups of hydroxyapatite is identified at slightly offset values compared to those in the FD spectrum, located at 1550, 1466 and 1392 cm^{-1} . New peaks of medium intensity from 1150, 840, 660 and a shoulder at 597 cm^{-1} were attributed to different phosphate and carbonate structures. These changes in frequency and intensity are attributed to the interaction of dentin with citric acid and the increase in the amount of water in the sample after immersion in citric acid. The peaks from 1704 and 1749 cm^{-1} present in the citric acid spectrum, are missing in the spectrum of the initial dentin, but appear after immersion in citric acid at 1702 and 1735 cm^{-1} . This indicates the progressive penetration of citric acid into the dentin structure as a function of immersion time. The presence of water inside the dentin after immersion is confirmed by the presence of a wide peak at 1632 cm^{-1} .

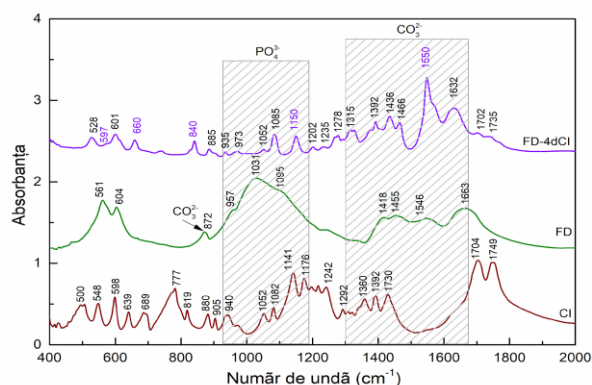


Figure 6.9. FTIR spectra in the range 400 - 2000 cm^{-1} for the initial dentine sample (FD) and after 4 days of immersion in citric acid (FD-4dCI), compared to the citric acid spectrum.

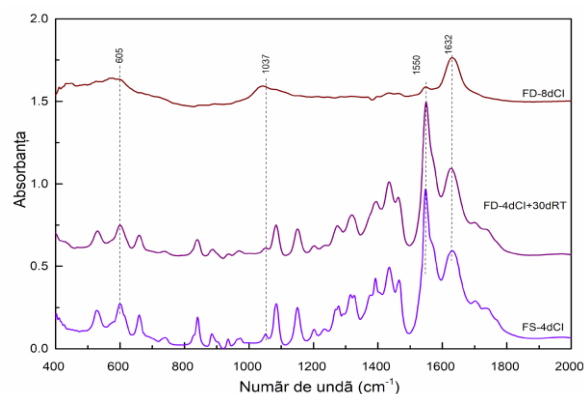


Figure 6.10. FT-IR spectra in the range 400–2000 cm^{-1} of the FD-4dCI sample after 30 days of storage at RT and after 8 days of immersion in citric acid.

The FT-IR spectrum of the dentine sample after 30 days of relaxation looks similar to the spectrum obtained before relaxation. Vibration bands occur without significant displacement or change in intensity. (Fig. 6.10) This indicates that the structure of the dentin does not deteriorate during this period of 30 days if the sample is maintained without the action of citric acid. Significant changes occur in the FD sample immersed for 8 days in citric acid. In the FT-IR spectrum bands are observed at 1632, 1550, 1037 and 605 cm^{-1} , and some vibration bands are missing or appear reduced in intensity, such as those at 660, 840, 1085, 1150, 1702, 1735 cm^{-1} . This indicates the strong effect of citric acid on the structure of the dentine after 8 days of immersion in acid.

6.3. Conclusions

From the XRD diffraction and FT-IR spectroscopy analyses on human tooth samples, the following conclusions can be drawn:

- X-ray diffractograms on the initial teeth show both an ordered phase -determined mainly by hydroxyapatite, as well as an amorphous phase determined by the organic components of the enamel. This structure remains almost unaffected after 4 days of immersion in citric acid. Preserving the samples in closed containers in the dark at room temperature for 30 days has no additional effect on their structure.
- If the total immersion period of the enamel in citric acid increases up to 8 days, due to the interaction of the enamel with citric acid, the ordered structure of the enamel is affected. From the X-ray diffractograms a decrease of the crystalline phase is observed. The structural changes in the enamel immersed for 4 days in citric acid are also confirmed by the FT-IR analysis, which identifies changes in the bonds at the molecular level. This process is amplified after a degradation of the sample in citric acid of 8 days. The presence of citric acid in the enamel structure is argued by identifying new vibration bands of citric acid.
- Diffractograms of dentine samples show a completely amorphous structure after 8 days in citric acid, which shows that these samples are more degraded than enamel samples. Degradation due to citric acid is also confirmed by FT-IR spectra, from which new vibration bands have been identified due to the presence of citric acid. The FT-IR spectrum of dentine samples is completely different compared to the spectrum of the initial sample, which indicates an acid penetration into the dentin structure and a chemical reaction with it.

In conclusion, it can be stated that enamel provides acceptable protection to the human tooth for a short time of exposure to citric acid, and dentin, without the protection of enamel, is strongly affected by citric acid.

Chapter 7: Final conclusions

The main objective was to investigate the effects of thermal, radiative, or chemical degradation in polymers. Three types of materials were studied: polystyrene, PET, and human teeth. This study is based on original results, which were first published in scientific journals. The following conclusions can be formulated after this research:

1. In the *commercial polystyrene* samples there are certain structural changes following the application of heat treatment. From the analysis of the measurements by X-ray diffraction, FT-IR spectroscopy, UV-VIS and fluorescence, on commercial polystyrene samples and on polystyrene samples heated to 150 °C, 200 °C, 250 °C, 300 °C and 350 °C respectively, it was highlighted that the heat treatment influences the arrangement of the polymer chains.

- From XRD analysis it was established that heating the polystyrene to 250 °C leads to a local rearrangement of the polymer chains in ordered structures. This effect is highlighted by increasing the intensity of the maximum diffraction peak and the value of the angle 2θ simultaneously with the increase in temperature. The increase of the crystalline phase percent occurs in the heated samples up to 250 °C, above this temperature the intensity of the maximum diffraction peak decreases, which indicates a destruction of the ordered phase and degradation of the polymer at a heat treatment of 300 °C and 350 °C, respectively. This effect is determined by the amplitude of the polymer chain dynamics with increasing thermal agitation and their rearrangement at different interplanetary distances compared to the state at lower temperatures. The interplanar distance "d" calculated for the initial polystyrene sample and for the polystyrene heated to 140 °C had the highest value of 4.98 Å, compared to the samples heated to higher temperatures where its value increases. Obtained for polystyrene heated to 200 °C and 250 °C $d = 4.74$ Å, and for samples heated to 300 °C and 350 °C $d = 4.55$ Å. The decrease of the interplanar distances with the increase of the heat treatment temperature of 300 - 350 °C indicates the destruction of the ordered phase through the oxidation and degradation process of polystyrene.

- The structural changes due to the heat treatment applied to the polystyrene were also confirmed by the thermal and thermogravimetric DTA / TGA analysis, which showed the stability of this material up to ~ 140 °C, and above this temperature it starts to decompose. The decomposition process continues at heating temperatures above 250 °C, an event that takes place simultaneously with the oxidation of the polymer, where the highest value of mass loss of 83% was obtained. If the material continues to heat up to temperatures above 500 °C, the decomposition and degradation of polystyrene continue.

- From the comparison of the FT-IR spectra obtained on the heated polystyrene samples with the spectrum of the initial unheated polystyrene sample, it was found that differences appear. The spectral bands characteristic of polystyrene are well defined and narrow. In the spectra of heat-treated polystyrene, some vibration bands characteristic of polystyrene disappear or others undergo changes in their amplitude. In the spectrum of the sample heated to 140 °C it is observed that in the spectral range 3000-2800 cm^{-1} , the bands due to the vibration of the CH group from 3060 and 3025 cm^{-1} disappear, and those from 2926 and 2854 cm^{-1} reduce their amplitude. In the low frequency region, the CH vibrations from 757, 698, and 539 cm^{-1} disappear, resulting in a structural organization

that modifies the local vicinity of the monomers by applying heat treatment. The spectrum of the sample heated to 200 and 250 °C looks similar to that of the sample heated to 140 °C. As the heating temperature of the samples increases up to 350°C, the bands disappear due to the vibration of the CH group from 2926 and 2854 cm⁻¹, which confirms the structural changes at high temperatures, due to the oxidation and decomposition processes of the material. These results are consistent with thermal and XRD analyses.

- In the case of *irradiated polystyrene samples*, we expect that following the absorption of gamma radiation, certain parts of the polymer chain will break, which will influence its dynamics and implicitly the local organization of the entire molecular assembly. From the analysis of the XRD diffractograms obtained on the irradiated and heated samples, a behavior similar to that of the heated but non-irradiated samples is observed, the polymer chains showing an ordering tendency up to temperatures of maximum 200 °C. Thus, by irradiating commercial polystyrene, there is a shift of the maximum diffraction peak to 2θ higher values, which leads to a decrease in the interplanar distance compared to the sample of unirradiated commercial polystyrene. Irradiation breaks the polymer chains and produces a more compact local rearrangement. Compared to the irradiated but not heat-treated sample, the diffractograms of the heat-treated samples up to 350 °C and then irradiated show similar behavior, after irradiation the maximum diffraction peak 2θ increases and shows a slight increase in intensity. Consequently, the interplanar distance decreases, a result that suggests the tendency of the rearrangement of polymer into a more compact structure. Due to the heat treatment applied to the samples before irradiation, the thermal agitation will increase and the short chains will have higher mobility than the long chains, which allows them an easier rearrangement in orderly structures. But increasing thermal agitation with increasing temperature also has a destructive effect on these ordered areas. We have two competing processes, on the one hand a tendency of order caused by a greater dynamics of the polymer chains and on the other hand a tendency of the destruction of these structures determined by the increase of the thermal agitation. But overall, the difference between the diffractograms of the irradiated and non-irradiated samples shows a clear effect of gamma irradiation on the polymer structure.

- Based on the UV-VIS absorption spectra obtained on thermally degraded polystyrene samples, it was established that the most efficient fluorescence excitation wavelengths are 315 nm, 340 nm and 365 nm. The spectra of the excited samples at different wavelengths contain signals with widths and amplitudes depending on the frequency of excitation, behavior correlated with the probabilities of transition between the electronic levels involved in fluorescence emission. The most important peak occurs at 409 nm regardless of the excitation frequency, but its amplitude depends on the excitation. Given the amplitude and width of this fluorescence peak, we consider 340 nm to be the most efficient excitation radiation. After heat treatment the position of the maximums of the fluorescence curves remains unchanged, but their amplitude and width depend on the temperature. At 200 °C the general appearance of the spectra is similar to that obtained for the unheated sample, whereas at 350 °C the amplitude of the peaks decreases dramatically due to the oxidation process of a part of the sample. However, the stable position of the fluorescence maxima suggests good stability of polystyrene even at high temperatures. This property can be taken into account in the technological processes of recycling these materials by heat treatment.

2. From the XRD analysis on the sample PET commercial - **G00**, it was established that it initially has a semi-crystalline structure, with a local order due to the parallel local arrangement of some portions of the polymer chain. After applying the melting-cooling heat treatment, the amplitude and position of the maximum diffraction change. Instead of the maximum diffraction peak from 25.5 ° in the initial PET diffractogram, in the heat-treated sample three broad, low intensity diffraction maxima are observed, located at 22.6, 26 and 43.5 °. This is explained by the fact that the polymer chains tend to decouple from the ordered state by diffusion or repetition, which leads to the appearance of new ordered domains, with interplanar distances different from those of the untreated sample. Thus, it is found that in the heat-treated sample there is a reduction of the ordered phase fraction and a decrease in the interplanetary distance from 3.48 Å in the initial sample to 3.42 Å in the molten-cooled PET. Based on the Gaussian function, the diffractograms for the peaks 22.6, 26 and 43.5° were simulated and it was obtained that after the heat treatment only 1.8% of the initial crystalline phase corresponding to the peak of 26° is preserved. The wide peak at 22.6° was due to the massive increase of the amorphous phase to 77 %, to the detriment of the initial crystalline phase, with the interplanar distance of 3.96 Å. The interplanar distances calculated for these angles confirmed that the heat treatment causes the cleavage of the polymer chains, the appearance of new crystallization centers and the decrease of the weight of the initial crystalline phase.

-XRD analysis of commercial PET samples - **G00**, and PET samples exposed to three doses of radiation - with the absorbed dose of samples of 465 Gy, 3 kGy and 7 kGy, showed that no major differences were observed compared to the non-irradiated sample, because the maximum diffraction also occurs at 25.5°. This means that at doses up to 7 kGy, only the polymer chains are cleaved, which adopts a disordered arrangement.

- The irradiation effect is more visible in melted-cooled and then irradiated PET samples. The maximum peak of diffraction which was in the sample G00 at 25.5°, appears in the diffractograms of the heat-treated and then irradiated samples, at lower values, at 22.6° and 21.6°, is much wider and decreases in amplitude. The destruction of the ordered phase is more pronounced in samples that before irradiation was subjected to heat-melting-cooling treatment, this effect increases as the absorbed dose is higher. As the irradiation dose increases, the value of the angle at which the maximum diffraction occurs decreases, and the peak at 43.5° decreases in intensity. From the simulation of the diffractogram obtained for the heat-treated PET and then irradiated at 3 kGy, it was shown that the widening of the diffraction line is due to the overlap of the peak from 26° with a new peak at 21.6° and another at 43.5°. By irradiation appears an ordered structure with the interplanar distance of 4.11 Å and 2.07 Å respectively corresponding to the peaks of 21.6° and 43.5°. The share of this ordered phase increases from the value of 70 % obtained for the heat-treated and non-irradiated sample, to 89% in the heat-treated and irradiated sample loa 3 kGy.

Similar to the study of the irradiated sample at 3 kGy, the parameters of the simulation of the diffractogram of the heat-treated sample and then irradiated at 7 kGy were determined. It was found that irradiation causes a decrease in the amplitude of all diffraction maxima, the disappearance of the peak from 26° represents the complete destruction of the ordered phase. After irradiation, only the phases from 21.6° and 43.5° remain. The share of the amorphous phase from 21.6° increases to 83.4 %, while the fraction of the phase due to the peak from 43.5° decreases to 16.6 %.

- DTA / TG measurements were performed on commercial PET, irradiated PET, melted-cooled PET at 300 °C and melted-cooled PET and then gamma irradiated with the absorbed dose of 7 kGy, highlighted the thermal events that

occur in the samples during heating up to 350 °C. The **G00 melted-cooled** has a behavior similar to that of the G00, the crystallization process starts at 150 °C, and after 200 °C the decomposition of the material begins. These results are consistent with the XRD analysis which indicated the presence of structural changes in heat-treated samples at over 200 °C. The thermal treatment by melting-cooling applied to PET samples, followed by gamma-irradiated, does not cause changes, except that the irradiation causes the polymer chains to break and organize them into several ordered structures, which leads to the broadening of the endothermic signal from 150 °C. This behavior is also adopted by the sample. heat treated and then gamma irradiated, in which the weight of the breaking of polymer chains increases due to the different dynamics of the chains, which favors the organization in ordered structures. The endothermic signal with the maximum temperature at 252 °C, is observed in all samples regardless of the degree of irradiation.

3. Measurements on samples of human teeth by X-ray diffraction and FT-IR spectroscopy, evaluated the structural stability of the enamel and dentine of the human tooth, in conditions of chemical degradation achieved by exposing the samples to the action of citric acid for different times regardless of the degree of irradiation.

- From the X-ray diffractogram obtained in the angular interval 2θ : 10 - 40° on the *enamel sample*, the amorphous phase of hydroxyapatite was identified, over which the crystalline phases of hydroxyapatite overlapped. The crystallographic planes were identified from the crystallographic database, to which the Miller indices were assigned. The analysis of the diffractogram obtained on the *enamel sample* immersed in citric acid for four days showed that in addition to the existing peaks before immersion, two new peaks appear, the first at 2θ : 40° corresponding to the presence of hydroxyapatite and the second peak at 2θ : 26.5° which was associated with citric acid (in CI it was at 26.1°). The fact that the peaks in the initial sample remained unchanged and only one line of citric acid was identified proves that the enamel acts as a protector and gives the tooth stability by allowing the acid to penetrate the enamel structure. If the action of citric acid is prolonged by immersing the tooth for 8 days in the citric acid solution, it was observed that the diffraction lines decrease in intensity and are shifted to higher values of the diffraction angle 2θ . These changes are due to the action of citric acid which begins to degrade the enamel entering the pores of the dentin. - Similar investigations were performed on the dentine sample. Compared to the diffraction lines of the enamel sample, dentine has wider diffraction lines, this is due to the very large difference between the crystallite size for the enamel sample ($D_{FS} \sim 50$ nm) and that of the dentin sample ($D_{FD} \sim 10$ nm). After immersing the sample with dentin in citric acid, the diffractograms show clear lines of pure citric acid after only 4 days of immersion. The presence of hydroxyapatite is observed, but some peaks disappear. This result shows that the tooth without enamel protection degrades much faster.

- After an immersion period of 8 days of the dentin sample in citric acid, there is an enlargement of the main diffraction lines, and the rest of the diffractogram becomes amorphous.

- From the analysis of FT-IR spectra on enamel and dentin samples before and after chemical degradation into citric acid, the characteristic vibrations of the PO_4^{3-} phosphate and CO_3^{2-} carbonate group were identified. After immersion in citric acid these vibrations appear at slightly modified values and in addition there are vibrations

characteristic of citric acid. In the dentin sample some vibrations disappear, this is due to the amorphization of the structure with the penetration of citric acid into the dentine structure.

- As a result of the study, it can be argued that enamel provides short protection for the human tooth from exposure to citric acid, and dentine, without the protection of enamel, teeth are strongly affected by citric

Selective references

1. J. P. Cohen Addad, "Physical properties of polymeric gels", Chichester (UK): John Wiley & Sons, (1996).
4. M. P. Gutierrez-Salazar and J. Reyes-Gasga, "Microhardness and chemical composition of human tooth", *Mater. Res.* 6, 367–373, (2003).
6. K. Mattox, *Biomaterials – Hard Tissue Repair and Replacement*, 3 (D. Muster, Editor), Elsevier, Amsterdam, (1992).
8. H. El Feki, J. M. Savariault and A. B. Salah, "Sodium-carbonate co-substituted hydroxyapatite ceramics", *J. Alloys Compd.* 287, 114–120 (1999).
9. R. Vasluianu, D. A. Forna, M. Zaltariov and A. Murariu, "In Vitro Study Using ATR-FTIR Method to Analyze the Effects of Carbamide Peroxide on the Dental Structure", *Rev. Chim.* 67, 2475–2478, (2016).
10. M. Constantiniuc, M. Muresan-Pop, M. Potara, M. Todica, A. Ispas, M. E. Barbinta-Patrascu, D. Popa "Spectral investigation of the stability of a photopolymerizable composite material", *J. Optoelectron. Adv. Mater.* 21, 740–745, (2019).
11. J. Reyes-Gasga, E. L. Martínez-Piñeiro, G. Rodríguez-Álvarez, G. E. Tiznado-Orozco, R. García-García and E. F. Brès, "XRD and FTIR crystallinity indices in sound human tooth enamel and synthetic hydroxyapatite", *Mater. Sci. Eng. C* 33, 4568–4574, (2013).
14. D. C. Bassett, *Principles of Polymer Morphology*, Cambridge (UK), Cambridge University Press, (1981).
15. X. F. Lu, J. N. Hay, Isothermal crystallization kinetics and melting behavior of poly(ethylene terephthalate), *Polymer* 42(23), 9423-9431, (2001).
17. M. Pop, S. Traian, L. Daraban, R. Fechete, "¹³C NMR study of gamma irradiated polystyrene", *Studia UBB Chemia*, 56, 129-134, (2011).
18. B. Demirel, A.H. Yaras, B.F. Elcicek, "Crystallization behavior of PET materials ", *Bil Enst Dergisi Cilt*; 13:26–35, (2011).
19. Mathew C. Celina, "Review of polymer oxidation and its relationship with materials performance and lifetime prediction, *Polymer Degradation and Stability*", 98(12), 2419-2429, (2013).
20. M. Todica, "Proprietăți fizice ale polimerilor", Cluj-Napoca, Presa Universitară Clujeană, ISBN 973-610-376-5, (2005).
21. B. Stuart, "Polymer Analysis". Chichester (UK), John Wiley & Sons, (2002).
22. S. A. Jabarín, "Crystallization kinetics of Polyethylene Terephthalate. II. Dynamic Crystallization of PET", *J. Appl. Polym. Sci.* 34, 97-102, (1987).
23. L. A. Baldenegro-Perez, D. Navarro-Rodríguez, F. J. Medellín-Rodríguez, B. S. Hsiao, C. A. Avila-Orta, I. Sics, "Molecular Weight and Crystallization Temperature Effects on Poly (ethylene terephthalate) (PET) Homopolymers, an Isothermal Crystallization Analysis", *Polym.* 6, 583, (2014).
25. S. Mouaci, N. Saidi-Amroun, V. Griseri, L. Berquez, G. Teysse, N. Belkah , M. Saidi, "Effect of Gamma Irradiation Dose on Space Charge in e-Beam Irradiated PET Films", (2019). IEEE Conference on Electrical Insulation and Dielectric Phenomena (CEIDP), Richland, United States. 777-780, (2019).
27. M. Todica L. Udrescu, G. Damian, S. Astilean, Spectroscopic investigation of PVA-TiO2 membranes gamma irradiated, *J. Mol. Struct.* 1044, 328, (2013).
28. M. Pop S. Traian, L. Daraban, R. Fechete, "¹³C NMR study of gamma irradiated polystyrene", *Stud. Chem.* 56, 129 (2011).
29. M. Rubinstein and R. Colby "Polymer Physics" Oxford (UK), Oxford University Press (2002).
30. J. R. Lakowicz, "Principles of Fluorescence Spectroscopy", Springer, (2006).
32. T. Iliescu, S. Pînzaru. "Spectroscopia Raman și SERS cu aplicații în biologie și medicină", Cluj-Napoca: Casa Cărții de Știință, ISBN: 978-973-133-887-3, (2011).
33. S. Aștilean, "Metode și tehnici moderne de spectroscopie optică", Cluj-Napoca: Casa Cărții de Știință, (2002).
36. M. Todica, L. Udrescu, "Metode experimentale în fizica polimerilor", Presa Universitară Clujeană, 56, (2013).

37. Shadi L. Malhotra, Jean Hesse, Louis-P Blanchard "Thermal decomposition of polystyrene", *Polymer*, 16(2), 81-93, (1975).
41. M. M. Radhi, A.J. Haider, Z.N. Jameel, T.W. Tee, M. Z.B. Rahman, A.B. Kassim, Synthesis and characterization of grafted acrylonitrile on polystyrene modified with activated carbon using gamma-irradiation. *Research Journal of Chemical Sciences*, 2(11), 1, (2012).
44. C. P. Ennis, R.I. Kaiser, "Mechanistical studies on the electron-induced degradation of polymers: polyethylene, polytetrafluoroethylene, and polystyrene", *Physical Chemistry Chemical Physics*, 12, 45, 14884, (2010).
46. B. Ahmed, S. K. Raghuvanshi, A. K. Srivastava, J. B. M. Krishna, M. A. Wahab, "Optical and structural study of aromatic polymers irradiated by gamma radiation", *Indian Journal of Pure Applied Physics*, 892-898 (2012)

Acknowledgements

This doctoral thesis was made with the support of some wonderful people with whom I have had the blessing of working with and to whom I am deeply grateful.

I want to thank the coordinator of this paper, Professor Dr. Todica Mihai for his support, encouragement, advice and patience. I am grateful for the knowledge he has shared, for his involvement and also for supporting me throughout my research period.

I want to thank the guidance committee consisting of Professor Dr. Simon Simion, Professor Dr. David Leontin, Associate Professor Dr. Turcu Flaviu for the discussions, interesting and valuable suggestions during the research period.

I want to thank professor dr. Ștefan Răzvan, dr. Olar Loredana and dr. Pop Viorel, from University of Agricultural Sciences and Veterinary Medicine in Cluj-Napoca, for their support in laboratory research, in the use of laboratory equipment, such as and for useful discussions.

I want to thank the researcher dr. Mureșan-Pop Marieta from the Institute for Interdisciplinary Research in Bio-Nano-Sciences, Babeș-Bolyai University, Cluj-Napoca, for her support, patience and constructive discussions during the research work.

I thank the Doctoral School of Physics for the opportunity given to follow the doctoral courses, a period that contributed to my professional and human development.

I also thank my loved ones who were in important moments, beautiful or hard, always by my side.

Last but not least, I want to thank my family for the support, understanding, encouragement and patience shown over the years. I am especially grateful to my mother and father for unconditionally supporting my entire development.